# SHORT-TERM EFFECT OF MECHANICAL LOADING ON THE CELL TRANSDIFFERENTIATION OF CONDYLAR CHONDROCYTES

A Thesis

by

AMANDA MITCHELL GROSS

Submitted to the Office of Graduate and Professional Studies of
Texas &M University
in partial fulfillment of the requirements for the degree of

MASTER OF SCIENCE

| | |
|---|---|
| Chair of Committee, | Yan Jing |
| Co-Chair of Committee, | Peter H. Buschang |
| Committee Members, | Jian Q. Feng |
| | Reginald W. Taylor |
| Head of Department, | Madhu K. Nair |

May 2021

Major Subject: Oral Biology

# ABSTRACT

Background:

Chondrocytes transdifferentiate into bone cells during condylar growth, but the regulation mechanism is unclear.

Purpose:

We aimed to investigate how mechanical loading affects chondrocyte-derived osteogenesis in condylar modeling.

Research Design:

Thirty-three Aggrecan-Cre$^{ERT2}$; R26R$^{tdTomato}$; 2.3Col1a1-GFP compound mice received tamoxifen injections at four-weeks-old and were divided into control and experimental groups. Appliances were bonded to shift the mandibles to the left for five days. Condylar analysis was performed using two-dimensional radiography, microcomputed tomography, and histomorphometry.

Results:

The experimental group developed asymmetric mandibles, with the protrusive side being longer than controls and the retrusive being shorter. The protrusive condyle showed an increase in cartilage matrix and chondrocyte-derived osteoblasts, especially in the posterior third. The reverse was shown on the retrusive side.

Conclusions:

Mechanical loading directly regulates condyle chondrogenesis and chondrocyte transdifferentiation, which affects the growth direction of the condyle.

ACKNOWLEDGEMENTS

I'd like to thank my committee members, Dr. Yan Jing, Dr. Peter Buschang, Dr. Jian Feng, and Dr. Reginald Taylor for their guidance and expertise regarding my project. I'd also like to thank Dania Alaraj, Dr. Ajay Shakya, Aileen To, Diane Chen, and Dr. Zheng Wang for all of their assistance in carrying out my project. This study would not have been possible without each of you.

I would also like to thank each member of the Class of 2021 – Drs. Jackson Savage, Brendan Hubbard, Lauren Brubaker, Brittany Spruiell, and Steven Leroy – for their friendship and support throughout residency. It's been a fun three years!

To my parents, Patrick and Lauren, thank you for your support and love that has helped get me through my education. I look up to both of you and am so grateful for all that you've done for me.

And finally, to my husband, Kyle, thank you for journeying life with me for the past seven years and being my biggest cheerleader. You're the best partner, cat parent, and soon-to-be father I could have ever asked for! And to Baby Gross, I hope we can instill a passion for education and research in you.

## CONTRIBUTORS AND FUNDING SOURCES

This work was supported by a thesis committee consisting of Drs. Yan Jing, Peter Buschang, and Reginald Taylor of the Department of Graduate Orthodontics and Dr. Jian Feng of the Department of Biomedical Sciences.

All work for the thesis was completed by the student, under the advisement and with assistance of Dr. Jing of the Department of Orthodontics.

This work was made possible by Dania Alaraj, Dr. Ajay Shakya, Aileen To, Diane Chen, and Dr. Zheng Wang for their contributions with data collection and in part by the Robert E. Gaylord Endowed Chair in Orthodontics.

NOMENCLATURE

| | |
|---|---|
| BrdU | 5-bromo-2'-deoxyuridine |
| CBCT | Cone-beam computed tomography |
| Co | Condylion |
| CoA | Anterior aspect of condyle |
| Col1a1 | Alpha chain of type I collagen |
| Col10a1 | Alpha chain of type X collagen |
| Col2 | Type II collagen |
| Comid | Condylion midpoint |
| $Con_{sup}$ | Superior aspect of the condyle |
| CoP | Posterior aspect of condyle |
| DAPI | 4′,6-diamidino-2-phenylindole |
| EDTA | Ethylenediaminetetraacetic acid |
| EdU | 5-Ethynyl-2′-deoxyuridine |
| GFP | Green fluorescent protein |
| Gn | Gnathion |
| IGF-1 | Insulin-like growth factor 1 |
| Ihh | Indian hedgehog homolog |
| Me | Menton |
| MF | Mental foramen |
| Osx | Osterix |
| Runx2 | Runt-related transcription factor 2 |
| TMJ | Temporomandibular joint |
| TRAP | Tartrate-resistant acid phosphatase |
| R26R | Rosa 26 Receptor |
| μCT | Microcomputed tomography |

TABLE OF CONTENTS

LIST OF FIGURES

LIST OF TABLES

# 1. LITERATURE REVIEW

## Introduction

To be successful in treating orthodontic patients, it is necessary for orthodontists to have a firm understanding on the craniofacial complex and how manipulation of growth and occlusion can optimize esthetics and function for our patients. During development, Buschang et al showed that the mandible is the least mature of the craniofacial bones and thus more easily affected by epigenetic factors and orthodontic treatment. The condyle plays a large role in how the mandible grows during adolescence, and therefore, how our patients present to us for treatment. A pivotal study was developed by Bjork and Skiller[1; 2] in 1972, in which they utilized implants to evaluate how the craniofacial complex grew in adolescents. In cases of more forward condylar growth, the mandible was shown to rotate counterclockwise, resulting in a more brachyfacial appearance; more posterior condylar growth resulted in clockwise rotation, creating a longer face and more deficient chin projection. Patients with skeletal malocclusions[3] and asymmetries[4] also show changes in condylar growth. For example, the growth of the condyles in class II div Is is found to be less overall and less vertical than class Is between 10 and 15 years of age.[3] The mandibles of class II patients are also found to be smaller than those of class I patients when measured from Co-Gn.[3; 5; 6] In class III patients, while excessive condyle growth has been shown to not be a causative factor, a more posterior growth direction of the condyle has been demonstrated, resulting in an increase in overall mandibular length.[1; 7; 8]

The ability to affect the rate and direction of condylar growth has intrigued orthodontists for decades. Studies on posterior intrusion[9] and functional appliances[10; 11] have shown effects on condylar growth. For example, many studies found that the use of a Bionator, Herbst, or Twin

block resulted in a statistically significant increase in mandibular length (measured as some variation of condylion/articulare to pogonion/gnathion) of approximately 1-2.5mm.[11] Anatomically, this increase was found to be due to increased posterior drift of the bone in the gonial region, more posteriorly directed condylar growth, and ultimately less true mandibular forward rotation than control patients.[10] Studies on posterior intrusion via methods involving miniscrews or high pull head gear have shown redirection of condylar growth in a forward direction, with reductions of the gonial angle and forward rotation of the mandible.[9]

While the anatomical differences in these adaptations have been noted, the cellular mechanics behind this adaptation is not fully understood. In order to optimally adapt the condyle, two questions must be answered. First, the exact mechanism of condylar growth needs to be understood, and second, how in which condylar growth can be manipulated.

The condyle grows via endochondral bone formation. Endochondral ossification begins as mesenchymal cells proliferate and differentiate into chondroblasts, which form hyaline cartilage. As the cartilage grows in size, chondroblasts become entrapped to become chondrocytes and hypertrophy. Blood vessels from the perichondrium bring osteoblasts to deposit a collar of bone around the cartilage. It is then thought, traditionally, that the collar of bone inhibits nutrients from diffusing to the center of cartilage, resulting in chondrocyte apoptosis and disintegration of the structure via osteoclasts from the periosteum. Blood vessels are then thought to penetrate the cavities and carry in them osteoprogenitor cells, which differentiate into osteoblasts to deposit bone.[12] This central dogma of endochondral ossification has been accepted for decades, suggesting that apoptosis of hypertrophic chondrocytes is necessary to initiate bone formation. [13; 14; 15 16]

While apoptosis has repeatedly been demonstrated in the deepest layers of hypertrophic chondrocytes, the extent of this phenomenon is debated.[17] Scientists have questioned whether hypertrophic chondrocytes indeed died after being released from the extracellular matrix or instead became osteoprogenitor cells, a hypothesis that dates back to the late 1800s with Van der Stricht[18] and Brachet.[12; 19] By using cell lineage tracing, an advanced technique to trace cell fate in vivo, several groups have recently proven that 60-70% of hypertrophic chondrocytes directly transdifferentiate into bone cells in the metaphysis. [20; 21; 22; 23; 24] Additionally, Jing et al, 2015 demonstrated that approximately 80% of bone cells in the condylar process arose via direct transformation of chondrocytes during prenatal growth.[25] These studies have clearly documented that chondrocytes play a critical role in endochondral bone formation, and that chondrogenesis and osteogenesis are one continuous process.

To date, however, the roles chondrocytes and their transformed bone cells play in condylar modeling remain largely unknown, especially during the alteration of mandibular position in orthodontic and orthopedic treatment. By creating a functional lateral shift of the mandible of mice similar to that of various studies,[26; 27; 28; 29] while using Jing's cell lineage tracing technique to assess chondrocyte transformation, we will have an opportunity to assess the novel roles of chondrocytes and their descendent cells in condylar growth. This evaluation will provide greater understanding of how condylar modeling is regulated by mechanical loading and shift our focus to hypertrophic chondrocytes as the key player in control of condylar growth, rather than the bone marrow through which the osteogenic cells were originally thought to come from. This new concept may open a new research direction relevant to the role of orthodontics in targeted condylar growth and regenerative therapies for TMJ degenerative diseases.

## Anatomy, Development, and Histology of the Mandibular Condyle

The condyle is the most posterior-superior process of the mandible. It is connected to temporal bone of the skull via the temporomandibular joint (TMJ), which allows for the mandibular movements necessary for daily life. The articular disc is positioned between the two bones, forming two spaces filled with synovial fluid: the superior and inferior joint cavities.[30] The TMJ is considered a ginglymoarthroidal joint, meaning it can undergo both rotational and translational movement.[31] Rotational movement occurs along inferior joint cavity, while translational movement occurs along the superior joint cavity.

The mandible begins development during the fifth week of fertilization, where a pair of Meckel's cartilages develop from the first branchial arch and appear along the mandibular nerves and vessels. Initial ossification of the mandible begins quickly after, such that bone forms via intramembranous ossification lateral to Meckel's cartilage. During the seventh week, a separate condylar blastema appears slightly distal but also adjacent to Meckel's cartilage. From weeks seven through fifteen, two distinctive growth patterns can then be observed: that of the mandibular body and that of the condyle. Intramembranous growth begins from the region of initial ossification and radiates outward to form the future mandibular body, ramus, coronoid, alveolar bone, and symphysis. Endochondral growth begins at the condylar blastema and grows conically in a posterior and vertical direction to form the mandibular condyle.[22]

Intramembranous and endochondral ossification differ in the many ways. Intramembranous ossification is characteristically formed in the flat bones of the face, the cranial bones, the clavicles, and the mandibular body.[32] Intramembranous growth is faster than endochondral growth and begins through the differentiation of mesenchymal cells into osteogenic cells. Growth is considered appositional, whereby new mesenchymal cells form new

bone, rather than osteoblasts differentiating into new osteoblasts.[12] Intramembranous ossification of the mandibular body follows four basic steps. Ossification begins through the development of an ossification center, where embryonic mesenchymal cells coalesce and begin to differentiate into specialized cells, namely osteogenic cells and capillaries. Differentiating osteoblasts produce osteoid, a fibrous matrix, which then becomes mineralized and entraps osteoblasts, inducing them to become osteocytes. Osteogenic cells in the surrounding connective tissue then differentiate into new osteoblasts at the edge of the bone. As time lapses, several clusters of osteoid unite around the capillaries to form a trabecular matrix, and osteoblasts on the surface become the cellular layer of periosteum. Finally, the periosteum secretes compact bone superficial to the spongy bone and the spongy bone condenses into red bone marrow.[12]

Contrastingly, endochondral ossification occurs in the bones at the base of the skull, long bones, and the condyle. The precursor cell of endochondral bone formation is cartilage, and tissue proliferation can occur either interstitially, as in primary cartilage formation through which the cartilage cells divide and proliferate, or appositionally, in which mesenchymal cells divide and subsequently differentiate into cartilage cells.[33] The central dogma of endochondral ossification is as shown in Figure 1a. Mesenchymal cells proliferate and differentiate into chondroblasts, which form hyaline cartilage. As the cartilage grows in size, chondroblasts become entrapped to become chondrocytes and hypertrophy. Blood vessels from the perichondrium bring osteoblasts to deposit a collar of bone around the cartilage. It is then thought, traditionally, that the collar of bone inhibits nutrients from diffusing to the center of cartilage, resulting in chondrocyte apoptosis and disintegration of the structure via osteoclasts from the periosteum.[12; 32] Blood vessels then penetrate the cavities and carry in them

osteoprogenitor cells, which differentiate into osteoblasts to deposit bone.[12] The thought has been that cartilage is thus replaced by bone, rather than bone forming directly from cartilage.[32]

Endochondral ossification can be segregated into two main types: primary and secondary. Primary ossification is found early in development as part of the primary skeletal cartilage and grows intrinsically in response to hormones. The chondrocytes themselves are the cells proliferating, causing interstitial growth, and the collagen composition is heavily type II.
The condyle is considered secondary cartilage. Secondary cartilage develops later in embryology and responds to local mechanical stimuli for growth. Growth is appositional where undifferentiated mesenchymal cells proliferate and follow by differentiating into cartilage cells, and the collagen composition consists of both type I and II collagen.[34; 35]

Histologically, the condylar cartilage is often categorized into layers, emulating its development. The top layer of the condylar cartilage is the fibrous layer, where static, flat cells run parallel to articular surface, functioning as a protective covering. The proliferative layer is next, consisting of irregularly shaped progenitor cells that are undergoing mitosis to supply cells for the lower layers. These cells then flatten as they differentiate from chondroblasts to chondrocytes. The third layer is the chondrocytic layer, which contains chondrocytes at various stages of maturation that deposit cartilage matrices. The cells enlarge in the hypertrophic cell layer, creating hypertrophic chondrocytes with cartilaginous matrix that adapts for mineralization.[16; 36] Growth in the cartilage is therefore due to 3 factors: cell addition, extracellular matrix deposition, and cellular enlargement.[16]

As stated, it has traditionally been accepted that endochondral bone formation in all areas of the body required apoptosis of hypertrophic chondrocytes to initiate bone cell recruitment and consequently bone formation.[13; 14; 15 16; 32] While apoptosis has repeatedly been demonstrated in

the deepest layers of hypertrophic chondrocytes, the extent of this phenomenon is debated.[17] Scientists have questioned whether hypertrophic chondrocytes indeed died after being released from the extracellular matrix or instead became osteoprogenitor cells, a hypothesis that dates back to the late 1800s with Van der Stricht[18] and Brachet.[12; 19] In 1967, Crelin and Koch evaluated the interpubic symphysial cartilage of mice fetuses and through autoradiography, confirmed that hypertrophic chondrocytes transformed into osteoblasts.[37] Additionally, Farnum et al., 1990 evaluated live cells in situ of rat growth plates and demonstrated through time-lapse cinemicroscopy and interference contrast microscopy that the last chondrocytes in columns were alive.[38] By using cell lineage tracing, an advanced technique to trace cell fate in vivo, several groups have recently proven that 60-70% of hypertrophic chondrocytes directly transdifferentiate into bone cells in the metaphysis.[20; 21; 22; 23; 24]

## Cell Tracing

Cell lineage tracing techniques provide a more rigorous way to study cell fate. Often a recombinase enzyme, which is only expressed in a specific type of cell, stimulates the expression of a reporter gene. In this way, these types of cells and their descendants are permanently labeled.[39] The Cre-loxP system is commonly used in lineage tracing. The Cre recombinase excises the STOP sequence and activates the reporter in the specific cell line when the mouse has both the Cre (the recombinase enzyme) and loxP expression. In some cases, the investigator can choose the favorable time point to activate the Cre with a drug such as tamoxifen if the Cre is fused to a modified form of the estrogen receptor ($Cre^{ERT2}$).[40] Fluorescent reporters have become standard in lineage tracing experiments since it can dramatically reduce the complexity and improve the accuracy and efficiency to trace the cell fate.[40; 41]

Prior to 2015, no studies had evaluated cell tracing in the condyle. Jing et al[25] in 2015 sought to prove that chondrocytes directly transdifferentiated into osteoblasts in pre- and post-natal condylar cartilage using cell lineage tracing in compound transgenic mice. Jing utilized two types of mice to prove to study the fate of condylar chondrocytes – one for embryonic development and one for postnatal development.

Jing's embryonic mice had three different mutations: Col10a1-Cre$^{ERT2}$, Rosa-26R$^{Tomato}$, and 2.3 Col1a1-GFP. In cells that contained collagen type 10 (that is, only hypertrophic chondrocytes), collagen type 10 and Cre would split. Cre$^{ERT2}$ then would be available to go into the nucleus and interact with the upstream inhibitor to the tomato gene, resulting in the tomato gene's activation. The gene tdTomato has been shown to have the brightest fluorescent proteins and strong epifluorescence, which makes it easily visualized with a bright red color.[39] In Jing's experimentation, the chondrocytes and all the cells derived from these chondrocytes would thus shine red. The 2.3 Col1a1-GFP is a genetically modified collagen type 1 that fluoresces green when expressed. Mature osteoblasts and osteoclasts contain this type of collagen type 1 and thus would shine green in their experiment. When all of the mouse lines were bred together, the red and green superimposed, leading to a yellow fluorescence. A yellow bone cell indicated the presence of both the tomato reporter and GFP, which demonstrated that the trans-differentiation of chondrocytes into bone cells had occurred. Jing divided the condylar process in three levels: superior, middle, and inferior. They then counted the number of red, yellow, and green cells in the different levels, finding that in the superior level, up to 80% of cells were red or yellow and thus derived from chondrocytes. In the middle, closer to 70% were red or yellow, and in the inferior section, only 40%, showing that bone formation in that area was not as much from the cartilage. This quantitative data again suggests that chondrocyte-derived bone cells are the main

cells to contribute to the endochondral bone formation.[25] Figure 1b outlines the new hypothesis of endochondral ossification.

Jing utilized a different line of mice for postnatal development. Their genotypes consisted of Aggrecan-Cre$^{ERT2}$, Rosa-26R$^{Tomato}$, and 2.3 Col1a1-GFP. Aggrecan-Cre$^{ERT2}$ is inducible, so at two weeks old, tamoxifen was injected into the mice to allow for analysis of newly formed cartilage following tamoxifen induction. Tamoxifen interrupts the interaction between Aggrecan and Cre$^{ERT2}$ in chondrocytes. Like the other mice triplicate, Cre$^{ERT2}$ can then go into the nucleus and interact with the inhibitor to the tomato gene, activating tomato. All the chondrocytes and chondrocyte-derived bone cells formed after initiation of experimentation would then shine red. The 2.3 Col1a1-GFP would fluoresce green when expressed without induction, so any osteoblasts and osteoclasts made from development until time of sacrifice would thus shine green. When all of the mouse lines are bred together, the red and green similarly superimposed, leading to a yellow fluorescence, demonstrating that the trans-differentiation of chondrocytes into bone cells during experimentation. Jing found that at 2-, 8-, and 14-days following tamoxifen injection that a gradual increase in red bone cells were found in the subchondral bone, thus supporting the notion that chondrocytes directly transdifferentiate into bone cells.

To date, however, the roles chondrocytes and their transformed bone cells play in condylar modeling remain largely unknown, especially during the alteration of mandibular position in orthodontic and orthopedic treatment. To trace the fate of chondrocytes in our experiment, we will use the Aggrecan-$^{CreERT2}$ line[42; 43] and cross it with R26R$^{tdTomato}$ mice, which will permanently label all the chondrocytes and their descendent cells after the injection of tamoxifen at four weeks old. To further confirm the osteogenic cell lineage of those chondrocyte-derived cells, we will combine the third mouse line, 2.3Col1a1-GFP, as many

investigators have shown that hypertrophic chondrocytes can differentiate into bone cells during development.[20; 21; 23; 25; 44]

## Condylar Adaptation

While the TMJ can form in the absence of extrinsic stimuli,[45] various studies have shown that maintaining the proliferating progenitor cells and the deposition of bone in the condylar process requires joint stimulation normally associated with function.[46; 47] Many studies have indicated that this growth has an adaptive capacity, particularly regarding the condylar cartilage in response to mechanical loading. Alteration of the position of mandibles has been evaluated in various ways to elucidate this adaptive capability. Assessment of both human and animal studies will illustrate what has been found regarding condylar adaptation.

### *Human Studies*

#### *Normal Development*

During development, Buschang et al[48] showed that the mandible is the least mature of the craniofacial bones and thus more easily affected by epigenetic factors and orthodontic treatment. The condyle plays a large role in how the mandible grows during adolescence, and therefore, how orthodontics patients present for treatment. A pivotal study was developed by Bjork and Skiller[1] in 1972, in which they utilized implants to evaluate how the craniofacial complex grew in adolescents. If superimposed on the anterior cranial base, they found that generally the condyle was displaced down and back while the mandible was displaced inferiorly and rotated forward, or counterclockwise. By superimposing on implants, they were able to illustrate true mandibular growth, showing that it usually resulted in a posterior deposition of bone at the ramus and generally an upward and either forward or backward curvature at the condyle. Many studies

have shown a high correlation between mandibular rotation and growth of the condyle.[1; 48] In cases of more forward condylar growth, the mandible was shown to rotate counterclockwise, thus bringing the chin forward; more posterior condylar growth resulted in clockwise rotation, creating a longer face and more deficient chin projection. The ratio of condylar growth has been shown to be approximately 8mm up and 1mm back,[49] with the average growth of the condyle at peak height velocity being approximately 2-3mm per year.

*Asymmetry*

Patients that have developed an asymmetry often have alterations that are detectable in both the mandible and condyle.[50] Schmid et al[51] found when evaluating adolescents with facial asymmetry and chin deviation that 75% had structural asymmetry while 10% had displacement. Functional asymmetries could result from the mandible being deflected laterally or antero-posteriorly if occlusal interferences inhibit the patient from occluding properly in centric relation.[50] It is probable to infer that if the interference is maintained for a significant period of time, functional asymmetries may lead to skeletal asymmetries, though significant evidence for this hypothesis is lacking in human data. You in 2010[22] evaluated 50 adults with skeletal class III due to mandibular prognathism using CBCTs. Twenty patients were symmetric and thirty asymmetric. You compared the differences in measurements between the two groups. On the non-deviated side or contralateral side of the asymmetric group (the side in which the chin is not going toward), You found that the condylar unit ($Con_{sup}$ to fossa of mandibular foramen) and the body unit (fossa of mandibular foramen to gonion midpoint) was longer and the ramal volume was larger.[52] Additionally, Lin et al[4] in 2013 evaluated 55 young adult patients with mandibular asymmetry, finding that condylar shape was altered. On the contralateral side, the condyle had a flatter anterior slope, a convex posterior slope, and a larger condylar size and volume. On the

ipsilateral side, they noted a more concave-convex condylar surface. These findings suggest that each condyle may adapt to its environment independently of the other.

*Skeletal Malocclusions*

Like asymmetric patients, patients with skeletal malocclusions also show deviations in mandibular and condylar growth.[3] For example, the growth of the condyles in class II div Is is found to be less overall and less vertical than class Is between 10 and 15 years of age.[3] The mandibles of class II patients are also found to be smaller than those of class I patients when measured from Co-Gn.[3; 5; 6] In class III patients, while excessive condyle growth has been shown to not be a causative factor, a more posterior growth direction of the condyle has been demonstrated, resulting in an increase in overall mandibular length.[1; 7; 8]

*Functional Appliances and Intrusion*

Studies on posterior intrusion[9] and functional appliances[10; 11; 53] have shown the adaptive effects of condylar growth and mandibular remodeling. For example, many studies found that the use of a Bionator, Herbst, or Twin block resulted in a statistically significant increase in mandibular length (measured as some variation of condylion/articulare to pogonion/gnathion) of approximately 1-2.5mm.[11] Anatomically, this increase was found to be due to increased posterior drift of the bone in the gonial region, more posteriorly directed condylar growth, and ultimately less true mandibular forward rotation than control patients.[10] Studies on posterior intrusion via methods involving miniscrews or high pull head gear have shown redirection of condylar growth in a forward direction, with reductions of the gonial angle and forward rotation of the mandible.[9]

***Animal studies:***

Many animal studies have been designed to evaluate the effects of various forms of mandibular adaptation. Primary adaptation mechanisms include protrusion, retrusion, forced opening/closing, and lateral shift, each of which will be assessed in detail.

*Protrusion*

The classic article illustrating condylar adaptation to the environment was performed by McNamara and Carlson in 1979. They found by creating a functional protrusion appliance to push the mandible of rhesus monkeys forward and down that in the posterior aspect of the condyle, the cartilage thickened and more bone was deposited.[54] Similar findings have been found in experiments on rats.[55; 56] Other studies have determined that with protrusion, first an increase in the prechondroblastic layer occurs, followed by increase in the hypertrophic layer and then endochondral condylar growth.[57; 58; 59; 60; 61] It is thought that advancement promotes stretching of the lateral pterygoid muscle fibers, causing the condyle to be more anteriorly positioned in the glenoid fossa and increases in cell responses and proliferation of blood vessels in the retrodiscal pad.[62; 63]

*Retrusion*

Cholasueksa in 2004 evaluated the effect of mandibular retrusion in rats using guiding appliances on the maxillary incisors, finding a decrease in cartilage and proliferative cells and a flattening along the posterior region.[64] Similar reductions in posterior condylar cartilage were found in other articles.[65; 66] Charlier and Petrovic (1967) evaluated the effect of chin cups on growing rats, finding that a week of use reduced the functional stimulus on the joint, causing slower proliferation and decreased thickness of the prechondroblast and chondroblast zones.[67] Petrovic proposed that the contraction of the lateral pterygoid muscle controls the rate of

proliferation of prechondroblasts, as he found that chin cup therapy caused decreased number of sarcomeres in the lateral pterygoid muscle and proliferation in the prechondroblastic zone, whereas hyperpropulsion increased them.[68]

*Altered Functional Loading*

Altered functional loading has been evaluated by various investigators. In 2009, Chen et al. trimmed the mandibular incisors of 3-week-old mice every other day for 2, 4, and 6 weeks to progressively decrease function. They found a significant reduction in the thickness of condylar cartilage.[69] Sobue et al (2011), Utreja et al. (2015), and Kaul et al. (2016) also evaluated altered loading through the use of springs to force 6-, 4-, and 4-week-old mice's mouths open for 1 hour/day for 5 days. With an increase in loading, all found an increase in mandibular condylar cartilage proliferation. However, Sobue et al found a significant increase in trabecular spacing and a decrease in bone volume fraction while Kaul et al found an increase in bone volume and decrease in trabecular spacing, a difference that may be explained by different strains, gender, and age of mice. [70; 71; 72] Thus, more studies are required to further demonstrate the effects and mechanisms of the loading alteration on the remodeling of condylar process.

*Lateral Shift*

The causal linkage between mandibular lateral displacement and changes in condylar modeling has been evaluated by many investigators. The main experimental methods and findings of twelve different studies are summarized in Table 1. The studies were performed on monkeys, rats, and mice. Different shifting mechanisms were used, including banding or bonding the maxillary incisors, banding the lower incisors, using bilaterally inclined mandibular splints, creating a fixation device screwed bilaterally into the zygomatic arch with an open coiled spring connected from the device to the mandibular incisors, or unilateral local injection of IGF-1, a

growth factor involved in regulation of endochondral ossification. The animals were evaluated anywhere between 3 days and 12 months. For the purposes of this paper, the ipsilateral side is defined as the side in which the mandible is shifting towards, with the contralateral side being the side in which the midline is shifting away from.

Table 2 summarizes the effects the twelve papers found regarding lateral deviation on mandibular and condylar morphology. The most common finding of the papers had to do with mandibular length, showing that the contralateral side was longer than the ipsilateral side. [74; 76; 77; 78; 79] Additionally, the contralateral side showed a shorter ramus height,[74; 76; 77] longer mandibular corpus, [76] shorter condylar AP length and narrower condylar width[79] from the frontal aspect. Thus, it appears that as a mandible shifts, we see should expect to see growth directed more posteriorly on the contralateral side, much like what appears to occur in functional appliances,[9] while the growth should be directed more vertically on the ipsilateral side.

These studies have also evaluated the condylar cartilage histologically. From an AP perspective, the studies have shown an increase in condylar cartilage thickness on the contralateral side,[27; 78] with most thickness concentrated along the posterior region.[78] Also noted on the contralateral side was an increase in the cell proliferation marker BrdU,[27] the osteogenic marker Runx2 and the chondrogenic markers Col2, Ihh, AKTF1, and Ki67.[78] Subchondral bone length also showed increases on the contralateral side, with overall new bone formation primarily being in the posterior aspect, while bone formation on the ipsilateral side was primarily anterior and superior.[77] This suggests that chondrogenesis and osteogenesis appear to be increased on the contralateral side, with particular increases focused on the posterior aspect. Ipsilateral bone formation appears to be more concentrated anteriorly and superiorly, mimicking the two-dimensional measurements evaluated grossly.

From a frontal perspective, the studies have shown an increase in condylar cartilage thickness on the contralateral side, particularly in the central region of the section.[28] The central aspect of the contralateral side was also associated with an increase in BrdU and a decrease in TRAP,[28] a molecule that stains osteoclasts, suggesting that cell proliferation is higher and bone degradation is lower in the central region on the contralateral side. Ishii et al did not separate the condylar section into segments, but found an expansion of the ”erosive zone” of bone on the contralateral side,[79] suggesting increased “erosion” of cartilage and bone formation as classified by Beresford and Phil in 1975.[80] The contralateral side also saw a narrowing of the neck. [79] On the ipsilateral side, chondrocytes shifted to the mesial aspect of the condyle, resulting in deformation of the mandibular neck and a lateral direction of ossification.[79] In the lateral region of the ipsilateral side, a decrease in condylar thickness and BrdU was also found, with an increase in TRAP,[28] suggesting that at least in the lateral aspect of the ipsilateral side, bone formation had decreased. Thus, from the frontal aspect we may anticipate that upon shifting, bone formation may increase moreso in the central region on the contralateral side, while on the ipsilateral side, bone formation appears to decrease in the lateral region and possibly be more focused on the medial side.

**Murine Condylar Growth**

Mice are often used as models for evaluating condylar growth. Mice are small, easy to handle, and quick to breed. Importantly, mice have been studied for decades and have the capability of gene modification, which allows for our project to occur. Specifics regarding murine condylar growth are important for experimentation and analysis and will be detailed here.

Murine condylar cartilage undergoes three phases of maturation. The first phase is between 6 and 8 weeks after birth, consisting of cartilage growth and endochondral ossification. The second phase continues until approximately 6 months of age, whereby mineralization and hyaline cartilage formation occurs to form the surface articular fibrocartilage. Cartilage then goes through a degenerative stage beyond 6 months of age.[81] Evaluating mandibular shape in mice, Swiderski et al (2013) concluded that mandibular shape matures later than size, with shape expected to reach 90% at age 27 days and 95% at age 35 days, compared to 18 days and 24 days for size, respectively. The condylar process were seen to elongate more than widen throughout growth, and cartilage caps in the condylar, coronoid, and angular processes were evident by at least 24 days old, with the sizes diminishing as the processes elongate.[39]

According to Flurkey, et al. (2007), the maturational rate of mice occurs 150 time faster during the first month of life and 45 times faster over the next five months than humans, in which they attain maturity at approximately 3-6 months (equivalent to 20-30 years of age for humans). [82] Four-week old mice are in a life phase equivalent for humans ranging from 9 to 11 years,[83] which is the gold therapeutic period for Class II or Class III orthopedic treatment. Thus, in the present, we will use 4-week old mice to establish the mandible alteration model, which may provide valuable evidence for the orthopedic treatment in adolescence.

## Study Aims

The primary objective of the study is to qualitatively and quantitatively determine the role and contribution of chondrocyte-derived bone cells in condylar remodeling by laterally shifting the mandible on mice. Our hypothesis for histological analysis is still such that endochondral ossification is different on the contralateral versus the ipsilateral side. We believe that in the posterior aspect we will find increased development and transformation of hypertrophic chondrocytes into osteogenic cells on the contralateral side. This should then prove that in condylar adaptation, hypertrophic chondrocytes are the key players in bone formation and thus the cells to focus on in potential control and adaptation of condylar growth rather than the bone marrow previously thought. Much is still unknown regarding the control mechanisms of condylar growth, and thus, our ability to manipulate it is still limited. Hopefully, with the help of this study, we can get one step closer to understanding condylar growth, so that one day, we can target the condyle in exactly the way we need to optimize treatment for our patients.

# 2. MATERIALS AND METHODS

## Samples

The experimental protocol was approved by the Institutional Animal Care and Use Committee of Texas A&M College of Dentistry, Dallas, TX (IACUC 2018-0138-CD, reference number 093679), and carried out in accordance with the guidelines for animal experimentation.

Thirty-three transgenic mice (Aggrecan-Cre$^{ERT}$; R26R$^{TdTomato}$; 2.3Col1a1-GFP) were obtained (provided by Feng lab at Texas A&M College of Dentistry) and cross bred to obtain the required genotypes. At four weeks of age (T1), the mice were divided into experimental (mandibular deviation, n=18) and control groups (no deviation, n=15). Four week old mice are pre-pubescent and equivalent to a human approximately 9 to 11 years of age.[83]

A pilot study was performed for five days using three mice before initiating the experiment to confirm experimental procedures, verify the stability of the lateral shifting model, and check mice viability. Mice were evaluated 1-2 times per day. Power analysis was performed using Kaul et al.'s (2016)[72] analysis using means and standard deviations of condyle head length and mandibular length. The minimum number to detect a 10% difference with a power of .9 and alpha of 0.05 was 15 mice per group.

## Experimental Procedures

All mice were anesthetized with an intraperitoneally administered Xylazine/Ketaset combination (Xylazine 1mg/mL; Ketaset 10mg/mL; 30 µL/body weight; as needed) following isoflurane inhalation and injected with 75 mg/kg of Tamoxifen intraperitoneally as a fluorescent label.

For the experimental group, bands were fabricated from 10μL Bioland Scientific LLC syringe tips to ensure consistent diameters and lengths that could be easily bondable to the mice's incisors (Figure 2). Measurements of the maxillary and mandibular bands were measured from the thinnest portion of the syringe. Cuts were made at 6mm and 8mm from the tip for a 2mm long mandibular incisor band. For the maxillary incisor band, cuts were made at 8mm and 11mm from the tip to make it cover the maxillary incisors entirely at 3mm long. Creation of the bands was done by the principal investigator with 3.0x loupes to ensure they were all the same size. The mouths of the mice were propped open using ligature ties secured into the surgical base and the incisors were isolated with cotton rolls. The mandibular incisors were then dried, primed with self-priming 3M™ Transbond™ Plus Self Etching Primer, dried again, the band was filled with FlowTrain Low Viscosity flowable composite resin, and cured at 430-480 nm blue light with a 3M UnitekTM OrtholuxTM Visible Light Curing Unit. The same steps were then applied for the maxillary incisors, ensuring parallelism to the mouse's midline. The mice's jaws were then actively shifted to the left (Figure 3). Band placement was performed by the same examiner to ensure application was similar across the shifting mice. The length and thickness of the bands ensured that the mice were unable to move their lower jaw out of its deviated position. No lateral deviation was performed on the control mice.

Following anesthesia, the mice received Buprenorphine 0.05-0.1mg/kg every 12 hours for at least 48 hours and more if the mouse was distressed. Mice were checked for signs of distress 2 to 3 times daily until fully recovered. Signs of distress included decrease in food and water intake, piloerection, hunched posture, weight loss, isolation and lack of movement. A weight loss of 20% or greater was considered catabolic and indicated a need for euthanasia. Mice were also evaluated daily to ensure proper hydration and nutrition, record the mice's weight, and

ensure maintenance of mandibular deviation. A graduated water cup was used to monitor water intake. All mice were fed a soft food diet starting at T1.

After five days (T2), all mice (18 experimental and 15 for control groups) were injected with EdU and sacrificed two hours later (timeline of 5 days verified from results obtained in Swiderski [39] and Fuentes et al[27]). For sacrifice, mice were anesthetized with a Xylazine/Ketaset combination (30ul/g) and anesthesia was confirmed by pinching the mouse's ankles. The mouse was deemed unconsciousness if it had no reactions. Cervical dislocation was proceeded for the sacrifice.

Radiographic Evaluation

All mice were fixated using 4% paraformaldehyde for 2 days in 4°C. Dissection of the mandible was performed to remove muscular tissue and mandibles were then hemisected along the mid-symphysis. Two-dimensional radiographs of the mandibles were captured using the Faxitron model MX-20 Specimen Radiography System (26 kV, 10 sec) with the labial surface of the bone lying flat on the base. For characterization of overall mandibular length, condylar head length, and condylar AP width, we had one blinded examiner measure the 2-dimensional X-rays as evaluated by Kaul et al[72] and shown in Figure 4. Nineteen were retraced two months later for reliability assessment. Reliability was assessed using intraclass correlations and method errors. Intraclass correlations were high for all two-dimensional analyses (Co-Me = .943, $p<0.001$; Comid-Me = .930, $p<0.001$; Comid-MF = .783, $p<0.001$; CoA-CoP = .822, $p<0.001$). Similarly, all method errors were deemed within the range of acceptability (Co-Me = .054mm, Comid-Me = .065mm, Comid-MF = .061mm, CoA-CoP = .049mm).

Micro-CTs were then taken of the mandible halves using the μCT 35 scanco medical machine with a voltage of 55 kV, exposure time of 0.8 seconds, and a current of 0.145 mA. Two regions of interest were traced for the μCT evaluations, including the superior 0.5 mm of the condyle and the condylar process superior to the mandibular foramen (Figure 5 a and b). One blinded examiner traced all condyles in the first manner, and a second blinded examiner traced all condyles in the second manner. The sectioned condyles were used to quantify the following trabecular bone properties: 1) apparent density, 2) material density, 3) tissue volume, 4) bone volume, 5) bone volume versus tissue volume, 6) trabecular number, 7) trabecular bone thickness; and 8) trabecular separation (similar evaluation performed in Kaul et al 2016).[72] All measurements were obtained directly from the μCT software. The μCT 3D image was then rotated to view the condyle from an inferior standpoint. A screen shot was captured as shown in Figure 5c and the frontal width of the condyle was evaluated by one blinded examiner.

Histological and Molecular Evaluations

Following radiographic evaluation, the ramus and condyle were cut from the corpus and the samples were submerged in a 4°C 10% EDTA bath for 5 days, dehydrated for 1 day in a 4°C 30% sucrose bath, and then embedded in optimal cutting temperature compound to prepare the samples for sectioning. The samples were sectioned (10 μm thick) along the sagittal plane with a cryosection machine. The sections for analysis were selected by one investigator along the mediolateral center where the AP width of the condyle was at its largest. Four sections were mounted on each slide for analysis.

A bright light microscope was used for toluidine blue staining analysis to qualitatively reflect the changes of condylar cartilage matrix production. A confocal microscope was used for

the fluorescent assessment of cell proliferation, immunostaining, and cell transdifferentiation. Fluorescent cell images were captured using the SP5 Leica confocal microscope. All images were captured at wavelengths ranging from 488 (green)-561 (red) μm. Multiple stacked images were taken at 200Hz and dimension of 1024x1024 using 10x or 20x glycerol objective lenses.

For quantitation of cartilaginous cell proliferation, intraperitoneal injections of EdU were administered 2 hours prior to sacrifice. EdU staining was performed following sectioning. Histomorphometric analyses was performed with Image-Pro plus 6.0 software. Total $EdU^+$ cell numbers were counted using ImageJ (as previously described in Jing et al, 2017).[17] To precisely investigate the effect of mandibular shifting on chondrocyte proliferation, the condylar cartilage was divided into anterior, middle, and posterior portions (Figure 6).[78] Cell proliferation rates were quantified by one blinded examiner for each of these three areas and for the total area in two ways: 1) as a measurement of EdU+ cells relative to the number of DAPI+ cells in the particular cartilaginous area (EdU+/DAPI+) and 2) as the number of EdU+ cells relative to the cartilaginous area itself (EdU+/area).

For quantification and detailed characterization of cartilaginous molecular changes, immunostaining was used to reflect the group differences in chondrogenesis.[25] Condyles were evaluated by one blinded examiner to assess the expression of the cartilaginous matrix markers Aggrecan and Col10a1. The condylar cartilage was also divided into anterior, middle, and posterior portions to quantify the areas of $Aggrecan^+$ and $Col10a1^+$ relative to the particular cartilaginous area ($marker^+$ area/area).

For quantification of cell transdifferentiation from chondrocytes into bone cells, the total number of red cells (that originated from $Aggrecan^+$ chondrocytes shining from expression of the red tomato gene), yellow cells (combination of red tomato, reflecting the chondrocyte origin, and

Osx or 2.3Col1a1-GFP, indicating the chondrocyte-derived bone cells), and green cells (chondrocyte-derived bone cells from either Osx or 2.3 Col1a1-GFP) in the condyle were counted using the Fiji/image J software by one blinded examiner. To determine if the proliferation of chondrocytes had a direct effect on the transformation of chondrocytes into bone cells during mandibular shifting, the condylar subchondral bone was again divided into anterior, middle, and posterior portions (Figure 4) to compare the numbers of chondrocyte-derived bone cells to the particular subchondral bone area (Aggrecan-Cre$^{+}$ and Osx$^{+}$ or Aggrecan-Cre$^{+}$ and 2.3Col1a1-GFP$^{+}$/area) in each group of mice and between groups.

Statistical Evaluation

Both mandibular halves (left and right) of the experimental group were evaluated except for two, whereby dissection resulted in fractures of the condylar head on the right side. One half (either right or left) was evaluated by the control group. All animals were evaluated for quantitative analysis, giving 34 mandibular halves/condyles to assess in the experimental group (18 left/retrusive, 16 right/protrusive) and 15 in the control group for a total of 49 mandibular halves/condyles.

Based upon skewness and kurtosis, some measurements were normally distributed, and some were not. All data regarding 2D morphometrics (mandibular length, condylar length, condylar width, frontal width), micro-CT measurements (distribution of bone volume, bone density, trabecular thickness, trabecular spacing), and Aggrecan and Col10a1 immunostaining were normally distributed. Data regarding analysis of EdU positive cells and number of cartilage-derived bone cells (using 2.3Col1a1-GFP and Osx) were not normally distributed. Data was compared in three manners, 1) protruded versus retruded, 2) protruded versus control, and 3)

retruded versus control. Two-dimensional morphometric data was evaluated using paired and student's t-tests. The right and left sides were evaluated with a paired t-test, but to account for the differences in weight at T2 between the experimental and control groups, analysis of covariance was performed. Immunostaining of Aggrecan and Col10a1 were evaluated using paired t-tests and independent t-tests, while cell proliferation and cell transdifferentiation with both GFP and Osx were analyzed with Wilcoxon and Mann-Whitney tests.

# 3. RESULTS

## Weight

There were no statistically significant between-group differences in weight at T1 (Table 3, Figure 7). At day 2, the experimental group was approximately two grams lighter than the control group, which was a statistically significant difference. Weight loss was slightly greater for the experimental than the control mice (3.0 g vs 2.1 g).

## Two-Dimensional Radiography Analysis: Mandibular Length, Condylar Length, Condylar AP and Frontal Width

The experimental group showed statistically significant between-side differences in the mandibular length (Co-Me and Comid-Me, $p<0.01$) and condylar length (Comid-MF, $p<0.05$) at the end of the experimental period (Table 4, Figure 8-9). The right (protrusive) side was longer than the left (retrusive) side in both measurements. After Bonferroni correction for multiple comparisons, there were no statistically significant between-group length differences (Table 5). There were also no statistically significant between-side or between-group differences in sagittal condylar width; however, condylar frontal width was significantly ($p<0.05$) smaller on the protrusive side of the experimental animals than the controls.

## Micro-CT Analysis: Apparent density, Material density, Tissue volume, Bone volume, Bone volume versus tissue volume, Trabecular number, Trabecular bone thickness, Trabecular separation

The apparent density of the superior 0.5 mm of the retrusive condyle was significantly ($p<0.01$) greater than the density of the protrusive condyle (Table 6, Figure 10), while the

material density of the condylar process was significantly ($p<0.05$) greater on the right compared to the left. The other measures showed no statistically significant between-side differences (Table 8, Figure 11-14). The control group had significantly higher apparent and material densities than the experimental group (Table 7 and 9, Figure 10). The control group also had greater absolute and relative bone volume than the experimental group, with the differences on the retrusive side attaining statistically significance. Finally, the control group had significantly more trabeculae, thicker trabeculae, and trabeculae that were closer together than the experimental groups.

Cell Proliferation: EdU

Cell proliferation in the protrusive condyle was significantly ($p<0.05$) greater than in the retrusive condyle, both for total area and that of the posterior third (Table 10 and 11, Figure 15-17). The anterior and middle areas showed the same patterns but no statistical significance.

For total area, the control showed significantly ($p<0.01$) less cell proliferation than the protrusive side of the experimental group (Table 12 and 13, Figure 15-17), but not significantly less than the retrusive side. In the posterior third of the condyle, the control group showed significantly less cell proliferation than both the protrusive ($p<0.01$) and retrusive ($p<0.05$) sides of the experimental group. No significant between-group differences were noted in the anterior or middle areas.

Chondrogenic Activity: Immunostaining for Aggrecan and Col10a1

Immunostaining for Aggrecan in the right (protrusive) condyle was significantly ($p<0.05$) greater than that of the retrusive condyle in the anterior, middle, posterior, and total areas of the

condylar cartilage (Table 14, Figure 18-19). Relative to the control group, the protrusive side had significantly ($p<0.05$) more Aggrecan immunostaining in the posterior third, but significantly less ($p<0.05$) in the middle third (Table 15). The left side had significantly ($p<0.01$) less aggrecan immunostaining relative to the control group in all aspects except the posterior third.

The protrusive condyle showed significantly ($p<0.05$) greater immunostaining for Col10a1 than the retrusive in the anterior, middle, posterior, and total condylar areas (Table 16, Figure 20-21). Relative to the control group, the protrusive side had significantly ($p<0.001$) more Col10a1 immunostaining in the anterior third (Table 17). The retrusive side showed significantly ($p<0.001$) less Col10a1 immunostaining than the control group in the total and middle third areas.

Cell Transdifferentiation: Quantitation of Aggrecan-Cre$^+$/Osx$^+$ cells and Aggrecan-Cre$^+$/2.3 Col1a1 GFP$^+$/ cells in subchondral bone

The protrusive condyle showed significantly ($p<0.001$) greater cell transdifferentiation of cartilage cells into Osx$^+$ bone cells (Aggrecan-Cre$^+$/Osx$^+$ cells) than the retrusive condyle in the anterior, middle, posterior, and total condylar areas (Table 18, Figure 22-23). There were no statistical differences between the control condyle and protrusive condyle of the experimental group (Table 19). The retrusive side showed significantly ($p<0.01$) less Aggrecan-Cre$^+$/Osx$^+$ cells than the controls for all areas.

There were no statistically significant side when evaluating the transdifferentiation of cartilage cells into 2.3 Col1a1$^+$ bone cells (Aggrecan-Cre$^+$/2.3 Col1a1 GFP$^+$ cells), though there was a trend toward higher differentiation on the protrusive than the retrusive sides (Table 20,

Figure 24-25). The control group had significantly ($p<0.05$) higher numbers of Aggrecan-$Cre^{+}$/2.3 Col1a1 $GFP^{+}$ cells than either side of the experimental group (Table 21).

# 4. DISCUSSION

A short-term sustained lateral shift of the mandible creates mandibular asymmetry, resulting in a longer mandibular length on the protrusive side (the side in which the mandible shifts away from) relative to the retrusive side. The present study showed that the mandibular length was 1.5% longer on the protrusive side relative to the retrusive side, with the controls having an intermediate length between the two. Other papers evaluating the effects of lateral shift on animals showed an increase in mandibular length on the protrusive side relative to the retrusive side.[26; 74; 76; 77; 78; 79] The differences in these articles related to the relationship of mandibular length to the control groups, finding either no significant differences between the control group and both sides,[78] a significant increase with only the protrusive side,[79] a significant decrease with only the retrusive side,[74; 77] or significant decreases with both sides.[76] These differences likely have to do with the mechanism of shifting, the number of experimental days, and the animal type and age. The increase in length on the protrusive side relative to the retrusive side is also consistent with studies on asymmetric patients, finding that the side in which the chin is not deviated toward has a longer mandibular length.[4; 52] A study on asymmetric patients also found a significant increase in condylar length on the protruded (or non-deviated) side, which was consistent with the 2.7% increase in condylar length on the protrusive versus retrusive sides, though the significance of the present study's results was not strong after Bonferroni corrections.[52] This finding suggests that protrusion of the condyle results in an evolutionary mechanism that stimulates condylar and thus mandibular growth, while the stimuli is decreased on the retrusive side.

Protrusion from lateral deviation appears to decrease the frontal and sagittal width of the condyle. The present study showed that the frontal width was 4.5% smaller and sagittal width

was 2.2% smaller on the protrusive side relative to the retrusive side. Our study did not find significant differences between sides or groups in AP condylar width, though the frontal width appeared significantly decreased on the protrusive side relative to the control group. This reduction in width is consistent with three studies in the sagittal analysis[74; 76; 78] and two in the frontal.[76; 79] This suggests that while the condyle certainly comes forward in protrusion, a lateral force likely from the surrounding ligaments and musculature is also in place, resulting in redirected growth to reduce the condylar width in both dimensions.

Over the short term, lateral deviation does not seem to produce significant bone mineralization changes evident at the micro-CT level between the protrusive or retrusive sides, though both appear to be less than control. The present study showed increased trabecular spacing and decreased bone density, volume, and trabeculation number/thickness of the experimental animals compared to the controls. Other studies noted similar results, reporting a decrease in condylar bone mineral density[29] and condylar bone volume, bone volume/total volume, and trabecular thickness[26; 76] in the experimental group relative to the control group. Two groups did note an even further decrease in condylar bone volume, bone surface, bone volume/tissue volume, trabecular thickness, and trabecular number on the protruded side relative to the retruded side.[26; 76] The authors postulated that loading was further decreased on the protruded side relative to the retruded side, resulting in decreased bone mineralization. The lack of significance in the right-to-left differences of the present study may be masked by the short experimental time and the significant weight loss observed during experimentation. Ultimately, the malocclusion in the present study likely caused a reduction in the masticatory demand on the teeth and masticatory muscles of the experimental group, affecting condylar bone maturation, mass, and quality.

Short-term protrusion from lateral deviation significantly increases chondrogenesis, especially in the posterior third. Factors from the present study contributing to such a conclusion are the increased cartilage proliferation, Aggrecan matrix production, and Collagen type 10a1 (Col10a1) matrix production on the protrusive side, especially in the posterior third. Other studies noted an increase in cartilage proliferation on the protrusive side,[27; 28; 78] using markers such as the thymidine analog 5-bromo-2-deoxyuridine (BrdU)[27; 28] and the monoclonal antibody Ki67.[78] Overall, this data is consistent with the present data using 5-ethynyl-2'-deoxyuridine (EdU), a thymidine analog similar to BrdU.[84] Although not previously used to study condylar adaptation to lateral deviation, Aggrecan and Col10a1 provide excellent markers for chondrogenic effects. Aggrecan is expressed by immature chondrocytes as a marker of chondrocyte differentiation, and Cola10a1 is an extracellular matrix protein expressed by early hypertrophic chondrocytes.[85] One study evaluated the effect of lateral deviation on chondrogenic markers, noting an increase in collagen type II (Col2) and Indian hedgehog (Ihh) on the protrusive side.[78] Col2, like Aggrecan, is another marker of chondrocyte differentiation expressed in immature chondrocytes, and Ihh is expressed when chondrocytes are moving from the pre-hypertrophic stage into early hypertrophic chondrocytes.[85] The increases in both Col2 and Ihh are consistent with increases with Aggrecan and Col10a1, showing increased chondrogenic activity on the protrusive side. While not evaluated in the present study, five animal studies evaluating lateral deviation also found a significant increase in condylar cartilage thickness[27; 28; 77; 78; 79] on the protrusive side, another sign of increased chondrogenesis. This increase was noted particularly in the posterior region from a sagittal perspective[77; 78] and the central region from a frontal perspective.[28] Taken together, one can presume that protrusion of

the condyle alters the biomechanical environment, resulting in increased stimulation of growth with increased chondrogenesis, particularly in the posterior aspect from a sagittal point of view.

Unlike the protrusive side, a short-term lateral shift of the mandible results in decreased chondrogenesis on the retrusive side. The results contributing to this conclusion are the decreased cartilage proliferation on the retrusive side relative to the protrusive side, and decreased Aggrecan and Col10a1 matrix production on the retrusive side relative to both the controls and protrusive side. Other studies have noted a decrease in BrdU on the retrusive side relative to the protrusive side,[27; 28] though one study noticed that for the first week, BrdU levels of the retrusive side were higher than that of the controls, much like the present data. However, they found after one week, the cell proliferation dropped significantly less than the controls and remained that way for the next three weeks of experimentation, attributing to the overall decrease in proliferation to increased compression forces.[28] No studies specifically documented the effect lateral shift had on chondrogenic markers in regards to the retrusive side. One study noted an increase in Col2 and Ihh on the protrusive side relative to the retrusive side, but since the source of protrusion in the study was a unilateral IGF-1 injection, true retrusion is unlikely on the opposite side. Nonetheless, retrusion from lateral deviation can be compared to the results from pure mandibular retrusion. One study reported the effects of mandibular retrusion on the condyle of rats, noting a decrease in type II collagen relative to the controls in the posterior condylar area, with even more pronounced decreases noted at days 30 and 60, supporting the notion that retrusion results in decreased chondrogenesis. Three lateral deviation studies also noted a decrease in condylar cartilage thickness on the retrusive side,[27; 28; 77] with particular decreases in the posterior third from a sagittal perspective[77] and the lateral third from a frontal perspective.[28] These findings further support the conclusions, suggesting that while cell proliferation increased

relative to controls in the short-term, increased compression forces from retrusion results in a decreased stimulation of chondrogenic growth.

The major finding of the present study is that a sustained lateral shift of the mandible for five days results in increased chondrocyte-derived osteogenesis on the protrusive side, particularly in the posterior region. This is a novel finding that otherwise has not been reported. Specifically, the present study showed significantly increased cell transdifferentiation with a higher number of chondrocyte-derived pre-osteoblasts (Aggrecan-Cre$^{+}$/Osx$^{+}$ cells) on the protrusive side relative to the retrusive side, especially in the posterior third of the condyle. Significant differences were not noted between the protrusive side and the control group, though the trends were present. Other studies have, however, reported an increase in osteogenesis on the protrusive side, detailed by either increased subchondral bone formation or increased osteoblastic transcription factors. For example, three studies noted an increase in subchondral bone formation on the protrusive side,[74; 77; 78] though one found the increase primarily in the anterior aspect of the condyle[78] while two found the increase to only be significant in the posterior aspect of the condyle.[74; 77] The increase in the anterior aspect likely has to do with the mechanism of shifting done in experimentation through unilateral injection of IGF-1.[78] The authors postulated that the induction at the anterior area was due to the abundance of IGF-receptors in the anterior area, which would explain why the anterior area was more induced than the posterior. Increased posterior bone formation is also found in animal studies with bilateral mandibular forward positioning.[56; 86] One study also noted an increase in the osteogenic marker Runx2, a transcription factor expressed by mesenchymal progenitors and required for full osteoblastic differentiation.[87] This induction further highlights the increase in osteogenesis on the protrusive side.

Cell lineage tracing helped clarify that a large part of the increase in osteogenesis on the protrusive side is due to the cartilage transitioning from cartilage to bone. Many investigators have shown that hypertrophic chondrocytes can differentiate into bone cells during normal development.[20; 21; 23; 25; 44] The mice in the study had an Aggrecan-Cre$^{ERT2}$ line[42; 43] crossed with R26R$^{tdTomato}$, which permanently labeled all the chondrocytes and their descendent cells after the injection of tamoxifen at four weeks old. To further confirm the osteogenic cell lineage of those chondrocyte-derived cells, the third mouse line was combined, using 2.3 Col1a1-GFP for one set of analysis and also using immunostaining for Osterix (Osx). Osx is genetically downstream of Runx2 and also an early transcription factor required for osteoblastogenesis.[87] Using Osx as the bone marker, the present study showed that five days was a long enough period to detect chondrocytes differentiating into pre-osteoblasts (Aggrecan-Cre$^{+}$/Osx$^{+}$ cells), thus elucidating the mechanism in which osteogenesis is affected during mandibular deviation. As osteoblasts continue to develop and differentiate, they produce the main bone constituent, collagen type I. Assessment of 2.3 Col1a1 targets the differentiation of mature osteoblasts to osteocytes. The study showed a significant decrease in development of chondrocyte-derived mature osteoblasts and osteocytes from the Aggrecan-Cre$^{+}$/2.3 Col1a1-GFP$^{+}$ cells in the experimental group relative to the control group. While the trend was still present that more Aggrecan-Cre$^{+}$/2.3 Col1a1-GFP$^{+}$ cells were noted on the protrusive side relative to the retrusive side, one can conclude that maturation was slowed in the experimental group and, therefore, five days was not enough time to detect a difference in the development of chondrocyte-derived mature bone cells after shifting. The decelerated maturation also helps explain why both sides of the experimental group had significant decreases in bone mineral content findings in the micro-CT analysis.

Short-term lateral shift of the mandible for five days results in decreased chondrocyte-derived pre-osteoblasts on the retrusive side, dictated by the significantly decreased Aggrecan-$Cre^{+}/Osx^{+}$ and Aggrecan-$Cre^{+}$/2.3 Col1a1-$GFP^{+}$ cells on the retrusive side relative to both the control group and the protrusive side. While, again, no studies have evaluated chondrocyte transdifferentiation in retrusion, two studies reported the amount of subchondral bone formation on the retruded side during lateral deviation.[74; 77] Both studies noted significantly decreased subchondral bone formation on the posterior aspect of the retruded side relative to the protruded side.[74; 77] However, unlike what our results would imply, Liu et al noted increased bone formation on the retruded side in the superior third,[74] while Stojic et al noted an increase in the anterior and superior thirds relative to the protruded side.[77] Liu et al evaluated the 4-week-old Wistar rats with the first set of evaluation being at 2 weeks. Stojic et al evaluated 5-week-old Wistar rats for 4 weeks. An explanation for such a discrepancy could be that the marked decrease in osteogenesis on the retrusive side is particularly evident during the first week of modeling, and later bone development and maturation catch up to the alterations in condylar position. Another possibility is that the bone deposited on the retrusive side is osteoblast-derived rather than chondrocyte-derived. Nonetheless, the results of the present study suggest that short-term compressive forces from retrusion due to lateral deviation result in decelerated chondrocyte transdifferentiation, and ultimately, decelerated growth.

The findings of this study are a mechanism of proof to show that in adolescent-aged mice, chondrocytes play a direct role in early bone modeling. Much like during fracture healing or accelerate bone growth, which can result in increased endochondral bone growth within 24 to 48 hours,[88] the present study has shown that cartilage responds quickly to lateral deviation by stimulating cell-transdifferentiation and growth in certain areas and decelerating in others. The

result of lateral deviation appears to affect the growth direction of the condyle, inducing a more posterior growth direction on the protrusive side and, at least, a less posterior growth direction on the retrusive side. This poses a question as to whether the condylar growth direction or amount could be controlled, with a new potential target being the differentiation of hypertrophic chondrocytes into bone cells.

Clinical Relevance

One area of clinical relevance has to do with the adaptability of the condyle to mandibular protrusion. Many studies found that the use of a Bionator, Herbst, or Twin block resulted in a statistically significant increase in mandibular length, with more growth being directed posteriorly.[11; 89; 90; 91; 92; 93; 94] At the molecular level, animal studies of pure protrusion discovered increased cartilage thickness and bone deposition.[54; 55; 56] With the findings from the present study, it can be further understood that class II functional appliances work initially by increasing chondrogenesis and chondrocyte-derived osteogenesis in a posterior growth direction, placing the emphasis of change on chondrocytes rather than independently developed osteoblasts.

Another area of clinical relevance has to do with the mechanism in which class III correctors like a chin cup or reverse-pull headgear work on the mandible. Deguchi and McNamara evaluated the craniofacial adaptations of chin cup therapy, finding mandibular length increased significantly less in the treated group compared to the control group.[2] Histologically, animal studies have found retrusion results in reductions in posterior condylar cartilage[64;65; 66] and slower proliferation.[67] Combined with the findings from the present study, it can be further understood that class III restrictive appliances appear to work initially by decreasing

chondrogenesis and chondrocyte-derived osteogenesis in the posterior direction, again emphasizing the importance of the cartilage response in initial growth changes.

The last area of clinical relevance for our study has to do with the development of mandibular asymmetry. As many studies have already elucidated,[26; 74; 76; 77; 78; 79] a lateral shift of the mandible results in a relative increase in posterior growth on the protrusive side and a relative decrease in the retrusive side that if left uncorrected, leads to skeletal asymmetry. This emphasizes the importance of correcting transverse issues early, such as with functional lateral crossbites.

# 5. CONCLUSIONS

A sustained lateral shift of the mandible for 5 days creates:

1. Mandibular asymmetry, resulting in a longer mandibular length and condylar length on the protrusive side relative to the retrusive side
2. Decreased mineralized bone content
3. An increase in chondrogenesis on the protrusive side, especially the posterior third
4. A decrease in chondrogenesis on the retrusive side
5. An increase in chondrocyte-derived osteogenesis (cell transdifferentiation) on the protrusive side, particularly in the posterior region
6. A decrease in chondrocyte-derived osteogenesis (cell transdifferentiation) on the retrusive side
7. An increase in posterior growth direction on the protrusive side
8. A decrease in posterior growth direction on the retrusive side

REFERENCES


1 BJÖRK, A.; SKIELLER, V. Facial development and tooth eruption. An implant study at the age of puberty. **Am J Orthod,** v. 62, n. 4, p. 339-83, Oct 1972. ISSN 0002-9416. Disponível em: < https://www.ncbi.nlm.nih.gov/pubmed/4506491 >.

2 DEGUCHI, T.; MCNAMARA, J. A. Craniofacial adaptations induced by chincup therapy in Class III patients. **Am J Orthod Dentofacial Orthop,** v. 115, n. 2, p. 175-82, Feb 1999. ISSN 0889-5406. Disponível em: < https://www.ncbi.nlm.nih.gov/pubmed/9971929 >.

3 JACOB, H. B.; BUSCHANG, P. H. Mandibular growth comparisons of Class I and Class II division 1 skeletofacial patterns. **Angle Orthod,** v. 84, n. 5, p. 755-61, Sep 2014. ISSN 1945-7103. Disponível em: < https://www.ncbi.nlm.nih.gov/pubmed/24524578 >.

4 LIN, H. et al. Mandibular asymmetry: a three-dimensional quantification of bilateral condyles. **Head Face Med,** v. 9, p. 42, Dec 2013. ISSN 1746-160X. Disponível em: < https://www.ncbi.nlm.nih.gov/pubmed/24354862 >.

5 NGAN, P. W.; BYCZEK, E.; SCHEICK, J. Longitudinal evaluation of growth changes in Class II division 1 subjects. **Semin Orthod,** v. 3, n. 4, p. 222-31, Dec 1997. ISSN 1073-8746. Disponível em: < https://www.ncbi.nlm.nih.gov/pubmed/9573884 >.

6 YOON, S. S.; CHUNG, C. H. Comparison of craniofacial growth of untreated Class I and Class II girls from ages 9 to 18 years: a longitudinal study. **Am J Orthod Dentofacial Orthop,** v. 147, n. 2, p. 190-6, Feb 2015. ISSN 1097-6752. Disponível em: < https://www.ncbi.nlm.nih.gov/pubmed/25636552 >.

7 WOLFE, S. M. et al. Craniofacial growth of Class III subjects six to sixteen years of age. **Angle Orthod,** v. 81, n. 2, p. 211-6, Mar 2011. ISSN 1945-7103. Disponível em: < https://www.ncbi.nlm.nih.gov/pubmed/21208071 >.

8 REYES, B. C.; BACCETTI, T.; MCNAMARA, J. A. An estimate of craniofacial growth in Class III malocclusion. **Angle Orthod,** v. 76, n. 4, p. 577-84, Jul 2006. ISSN 0003-3219. Disponível em: < https://www.ncbi.nlm.nih.gov/pubmed/16808562 >.

9 BUSCHANG, P. H.; CARRILLO, R.; ROSSOUW, P. E. Orthopedic correction of growing hyperdivergent, retrognathic patients with miniscrew implants. **J Oral Maxillofac Surg,** v. 69, n. 3, p. 754-62, Mar 2011. ISSN 1531-5053. Disponível em: < https://www.ncbi.nlm.nih.gov/pubmed/21236539 >.

10 ARAUJO, A. M.; BUSCHANG, P. H.; MELO, A. C. Adaptive condylar growth and mandibular remodelling changes with bionator therapy--an implant study. **Eur J Orthod,** v. 26, n. 5, p. 515-22, Oct 2004. ISSN 0141-5387. Disponível em: < https://www.ncbi.nlm.nih.gov/pubmed/15536840 >.

11 MEIKLE, M. C. Remodeling the dentofacial skeleton: the biological basis of orthodontics and dentofacial orthopedics. **J Dent Res,** v. 86, n. 1, p. 12-24, Jan 2007. ISSN 0022-0345. Disponível em: < https://www.ncbi.nlm.nih.gov/pubmed/17189458 >.

12 HALL, B. K. **Bones and Cartilage: Developmental and Evolutionary Skeletal Biology**. Second. London, UK: British Poultry Science, 2015.

13 CANCEDDA, R. et al. Developmental control of chondrogenesis and osteogenesis. **Int J Dev Biol,** v. 44, n. 6, p. 707-14, 2000. ISSN 0214-6282. Disponível em: < https://www.ncbi.nlm.nih.gov/pubmed/11061435 >.

14 GARANT, P. R. **Oral Cells and Tissues**. Germany: Quintessence Publishing, 2003.

15 GARTNER, L. P.; HIATT, J. L. **Color Textbook of Histology**. Philadelphia: Saunders, 1997.

16 LUDER, H. U.; LEBLOND, C. P.; VON DER MARK, K. Cellular stages in cartilage formation as revealed by morphometry, radioautography and type II collagen immunostaining of the mandibular condyle from weanling rats. **Am J Anat,** v. 182, n. 3, p. 197-214, Jul 1988. ISSN 0002-9106. Disponível em: < https://www.ncbi.nlm.nih.gov/pubmed/3213819 >.

17 HINTON, R. J. et al. Role of Chondrocytes in Endochondral Bone Formation and Fracture Repair. **Journal of Dental Research,** v. 96, n. 1, p. 23-30, 2017.

18 VAN DER STRICHT, O. Recherches sur le cartilage articulaire des oiseaux. **Archives of Biological Sciences,** v. 10, p. 1-41, 1890.

19 BRACHET, A. Etude sur la resoprtion des cartilages et la developpement des os longs chez les oiseaux. **Int. Monatsschr. Anat. Physiol.**, p. 391-417, 1983.

20 YANG, L. et al. Hypertrophic chondrocytes can become osteoblasts and osteocytes in endochondral bone formation. **Proc Natl Acad Sci U S A,** v. 111, n. 33, p. 12097-102, Aug 2014. ISSN 1091-6490. Disponível em: < https://www.ncbi.nlm.nih.gov/pubmed/25092332 >.

21 YANG, G. et al. Osteogenic fate of hypertrophic chondrocytes. **Cell Res,** v. 24, n. 10, p. 1266-9, Oct 2014. ISSN 1748-7838. Disponível em: < https://www.ncbi.nlm.nih.gov/pubmed/25145361 >.

22 LEE, S. K. et al. Prenatal development of the human mandible. **Anat Rec,** v. 263, n. 3, p. 314-25, 07 2001. ISSN 0003-276X. Disponível em: < https://www.ncbi.nlm.nih.gov/pubmed/11455541 >.

23 ZHOU, X. et al. Chondrocytes transdifferentiate into osteoblasts in endochondral bone during development, postnatal growth and fracture healing in mice. **PLoS Genet,** v. 10,

n. 12, p. e1004820, Dec 2014. ISSN 1553-7404. Disponível em: < https://www.ncbi.nlm.nih.gov/pubmed/25474590 >.

24 PARK, J. et al. Dual pathways to endochondral osteoblasts: a novel chondrocyte-derived osteoprogenitor cell identified in hypertrophic cartilage. **Biol Open,** v. 4, n. 5, p. 608-21, Apr 2015. ISSN 2046-6390. Disponível em: < https://www.ncbi.nlm.nih.gov/pubmed/25882555 >.

25 JING, Y. et al. Chondrocytes Directly Transform into Bone Cells in Mandibular Condyle Growth. **J Dent Res,** v. 94, n. 12, p. 1668-75, Dec 2015. ISSN 1544-0591. Disponível em: < https://www.ncbi.nlm.nih.gov/pubmed/26341973 >.

26 NAKANO, H. et al. Micro X-ray computed tomography analysis for the evaluation of asymmetrical condylar growth in the rat. **Orthod Craniofac Res,** v. 6 Suppl 1, p. 168-72; discussion 179-82, 2003. ISSN 1601-6335. Disponível em: < https://www.ncbi.nlm.nih.gov/pubmed/14606552 >.

27 FUENTES, M. A. et al. Lateral functional shift of the mandible: Part I. Effects on condylar cartilage thickness and proliferation. **Am J Orthod Dentofacial Orthop,** v. 123, n. 2, p. 153-9, Feb 2003. ISSN 0889-5406. Disponível em: < https://www.ncbi.nlm.nih.gov/pubmed/12594421 >.

28 SATO, C.; MURAMOTO, T.; SOMA, K. Functional lateral deviation of the mandible and its positional recovery on the rat condylar cartilage during the growth period. **Angle Orthod,** v. 76, n. 4, p. 591-7, Jul 2006. ISSN 0003-3219. Disponível em: < https://www.ncbi.nlm.nih.gov/pubmed/16808564 >.

29 NAKAMURA, A. et al. Influence of malocclusion on the development of masticatory function and mandibular growth. **Angle Orthod,** v. 83, n. 5, p. 749-57, Sep 2013. ISSN 1945-7103. Disponível em: < https://www.ncbi.nlm.nih.gov/pubmed/23327417 >.

30 OKESON, J. **Management of Temporomandibular Disorders and Occlusion**. 1989.

31 WADHWA, S.; KAPILA, S. TMJ disorders: future innovations in diagnostics and therapeutics. **J Dent Educ,** v. 72, n. 8, p. 930-47, Aug 2008. ISSN 0022-0337. Disponível em: < https://www.ncbi.nlm.nih.gov/pubmed/18676802 >.

32 GILBERT, S. **Developmental Biology**. Osteogenesis: The Development of Bones. ASSOCIATES, S. M. S. https://www.ncbi.nlm.nih.gov/books/NBK10056/ 2000.

33 COLLEGE, O. **Anatomy & Physiology**. Houston, TX: OpenStax CNX 2013.

34 MÉRIDA VELASCO, J. R. et al. Development of the mandibular condylar cartilage in human specimens of 10-15 weeks' gestation. **J Anat,** v. 214, n. 1, p. 56-64, Jan 2009. ISSN 1469-7580. Disponível em: < https://www.ncbi.nlm.nih.gov/pubmed/19166473 >.

[35] DELATTE, M. et al. Primary and secondary cartilages of the neonatal rat: the femoral head and the mandibular condyle. **Eur J Oral Sci,** v. 112, n. 2, p. 156-62, Apr 2004. ISSN 0909-8836. Disponível em: < https://www.ncbi.nlm.nih.gov/pubmed/15056113 >.

[36] MIZOGUCHI, I.; TORIYA, N.; NAKAO, Y. **Growth of the mandible and biological characteristics of the mandibular condylar cartilage**: Japanese Dental Science Review. 49**:** 139-150 p. 2013.

[37] CRELIN, E. S.; KOCH, W. E. An autoradiographic study of chondrocyte transformation into chondroclasts and osteocytes during bone formation in vitro. **Anat Rec,** v. 158, n. 4, p. 473-83, Aug 1967. ISSN 0003-276X. Disponível em: < https://www.ncbi.nlm.nih.gov/pubmed/6055085 >.

[38] FARNUM, C. E.; TURGAI, J.; WILSMAN, N. J. Visualization of living terminal hypertrophic chondrocytes of growth plate cartilage in situ by differential interference contrast microscopy and time-lapse cinematography. **J Orthop Res,** v. 8, n. 5, p. 750-63, Sep 1990. ISSN 0736-0266. Disponível em: < https://www.ncbi.nlm.nih.gov/pubmed/2201757 >.

[39] SWIDERSKI, D. L.; ZELDITCH, M. L. The complex ontogenetic trajectory of mandibular shape in a laboratory mouse. **J Anat,** v. 223, n. 6, p. 568-80, Dec 2013. ISSN 1469-7580. Disponível em: < https://www.ncbi.nlm.nih.gov/pubmed/24111948 >.

[40] HUMPHREYS, B. D.; DIROCCO, D. P. Lineage-tracing methods and the kidney. **Kidney Int,** v. 86, n. 3, p. 481-8, Sep 2014. ISSN 1523-1755. Disponível em: < https://www.ncbi.nlm.nih.gov/pubmed/24088959 >.

[41] ROMAGNANI, P.; RINKEVICH, Y.; DEKEL, B. The use of lineage tracing to study kidney injury and regeneration. **Nat Rev Nephrol,** v. 11, n. 7, p. 420-31, Jul 2015. ISSN 1759-507X. Disponível em: < https://www.ncbi.nlm.nih.gov/pubmed/25963592 >.

[42] AKIYAMA, H. et al. Osteo-chondroprogenitor cells are derived from Sox9 expressing precursors. **Proc Natl Acad Sci U S A,** v. 102, n. 41, p. 14665-70, Oct 2005. ISSN 0027-8424. Disponível em: < https://www.ncbi.nlm.nih.gov/pubmed/16203988 >.

[43] HENRY, S. P. et al. Generation of aggrecan-CreERT2 knockin mice for inducible Cre activity in adult cartilage. **Genesis,** v. 47, n. 12, p. 805-14, Dec 2009. ISSN 1526-968X. Disponível em: < https://www.ncbi.nlm.nih.gov/pubmed/19830818 >.

[44] PURCELL, P.; TRAINOR, P. A. The Mighty Chondrocyte: No Bones about It. **J Dent Res,** v. 94, n. 12, p. 1625-7, Dec 2015. ISSN 1544-0591. Disponível em: < https://www.ncbi.nlm.nih.gov/pubmed/26341975 >.

[45] GLASSTONE, S. Differentiation of the mouse embryonic mandible and squamo-mandibular joint in organ culture. **Arch Oral Biol,** v. 16, n. 7, p. 723-9, Jul 1971. ISSN 0003-9969. Disponível em: < https://www.ncbi.nlm.nih.gov/pubmed/5283530 >.

[46] ABE, K.; TAKATA, M.; KAWAMURA, Y. A study on inhibition of masseteric -motor fibre discharges by mechanical stimulation of the temporomandibular joint in the cat. **Arch Oral Biol,** v. 18, n. 2, p. 301-4, Feb 1973. ISSN 0003-9969. Disponível em: < https://www.ncbi.nlm.nih.gov/pubmed/4515594 >.

[47] DUTERLOO, H. S.; WOLTERS, J. M. Experiments on the significance of articular function as a stimulating chondrogenic factor for the growth of secondary cartilages of the rat mandible. **Trans Eur Orthod Soc**, p. 103-15, 1971. Disponível em: < https://www.ncbi.nlm.nih.gov/pubmed/5293075 >.

[48] BUSCHANG, P. H.; BAUME, R. M.; NASS, G. G. A craniofacial growth maturity gradient for males and females between 4 and 16 years of age. **Am J Phys Anthropol,** v. 61, n. 3, p. 373-81, Jul 1983. ISSN 0002-9483. Disponível em: < https://www.ncbi.nlm.nih.gov/pubmed/6614151 >.

[49] BUSCHANG, P. H.; SANTOS-PINTO, A. Condylar growth and glenoid fossa displacement during childhood and adolescence. **Am J Orthod Dentofacial Orthop,** v. 113, n. 4, p. 437-42, Apr 1998. ISSN 0889-5406. Disponível em: < https://www.ncbi.nlm.nih.gov/pubmed/9563360 >.

[50] BISHARA, S. E.; BURKEY, P. S.; KHAROUF, J. G. Dental and facial asymmetries: a review. **Angle Orthod,** v. 64, n. 2, p. 89-98, 1994. ISSN 0003-3219. Disponível em: < https://www.ncbi.nlm.nih.gov/pubmed/8010527 >.

[51] SCHMID, W.; MONGINI, F.; FELISIO, A. A computer-based assessment of structural and displacement asymmetries of the mandible. **Am J Orthod Dentofacial Orthop,** v. 100, n. 1, p. 19-34, Jul 1991. ISSN 0889-5406. Disponível em: < https://www.ncbi.nlm.nih.gov/pubmed/2069142 >.

[52] YOU, K. H. et al. Three-dimensional computed tomography analysis of mandibular morphology in patients with facial asymmetry and mandibular prognathism. **Am J Orthod Dentofacial Orthop,** v. 138, n. 5, p. 540.e1-8; discussion 540-1, Nov 2010. ISSN 1097-6752. Disponível em: < https://www.ncbi.nlm.nih.gov/pubmed/21055584 >.

[53] SANKEY, W. L. et al. Early treatment of vertical skeletal dysplasia: the hyperdivergent phenotype. **Am J Orthod Dentofacial Orthop,** v. 118, n. 3, p. 317-27, Sep 2000. ISSN 0889-5406. Disponível em: < https://www.ncbi.nlm.nih.gov/pubmed/10982934 >.

[54] MCNAMARA, J. A.; CARLSON, D. S. Quantitative analysis of temporomandibular joint adaptations to protrusive function. **Am J Orthod,** v. 76, n. 6, p. 593-611, Dec 1979. ISSN 0002-9416. Disponível em: < https://www.ncbi.nlm.nih.gov/pubmed/117715 >.

[55] GHAFARI, J.; DEGROOTE, C. Condylar cartilage response to continuous mandibular displacement in the rat. **Angle Orthod,** v. 56, n. 1, p. 49-57, Jan 1986. ISSN 0003-3219. Disponível em: < https://www.ncbi.nlm.nih.gov/pubmed/3082256 >.

[56] RABIE, A. B.; SHE, T. T.; HÄGG, U. Functional appliance therapy accelerates and enhances condylar growth. **Am J Orthod Dentofacial Orthop,** v. 123, n. 1, p. 40-8, Jan 2003. ISSN 0889-5406. Disponível em: < https://www.ncbi.nlm.nih.gov/pubmed/12532062 >.

[57] CHARLIER, J. P.; PETROVIC, A.; HERRMANN-STUTZMANN, J. Effects of mandibular hyperpropulsion on the prechondroblastic zone of young rat condyle. **Am J Orthod,** v. 55, n. 1, p. 71-4, Jan 1969. ISSN 0002-9416. Disponível em: < https://www.ncbi.nlm.nih.gov/pubmed/5248058 >.

[58] PETROVIC, A. G. Mechanisms and regulation of mandibular condylar growth. **Acta Morphol Neerl Scand,** v. 10, n. 1, p. 25-34, Oct 1972. ISSN 0001-6225. Disponível em: < https://www.ncbi.nlm.nih.gov/pubmed/4643663 >.

[59] STUTZMANN, J.; PETROVIC, A. Intrinsic regulation of the condylar cartilage growth rate. **Eur J Orthod,** v. 1, n. 1, p. 41-54, 1979. ISSN 0141-5387. Disponível em: < https://www.ncbi.nlm.nih.gov/pubmed/296928 >.

[60] VARDIMON, A. D. et al. Functional orthopedic magnetic appliance (FOMA) II--modus operandi. **Am J Orthod Dentofacial Orthop,** v. 95, n. 5, p. 371-87, May 1989. ISSN 0889-5406. Disponível em: < https://www.ncbi.nlm.nih.gov/pubmed/2718968 >.

[61] DE SÁ, M. P. N. et al. Histological and morphological evaluation of condylar cartilage of young rats in response to stimulation of mandibular protrusion. **Maringá,** v. 39, n. July-December, p. 219-226, 2017.

[62] RABIE, A. B.; HÄGG, U. Factors regulating mandibular condylar growth. **Am J Orthod Dentofacial Orthop,** v. 122, n. 4, p. 401-9, Oct 2002. ISSN 0889-5406. Disponível em: < https://www.ncbi.nlm.nih.gov/pubmed/12411886 >.

[63] LEUNG, F. Y.; RABIE, A. B.; HÄGG, U. Neovascularization and bone formation in the condyle during stepwise mandibular advancement. **Eur J Orthod,** v. 26, n. 2, p. 137-41, Apr 2004. ISSN 0141-5387. Disponível em: < https://www.ncbi.nlm.nih.gov/pubmed/15130035 >.

[64] CHOLASUEKSA, P.; WARITA, H.; SOMA, K. Alterations of the rat temporomandibular joint in functional posterior displacement of the mandible. **Angle Orthod,** v. 74, n. 5, p. 677-83, Oct 2004. ISSN 0003-3219. Disponível em: < https://www.ncbi.nlm.nih.gov/pubmed/15529504 >.

[65] TERAMOTO, M. et al. Effect of compressive forces on extracellular matrix in rat mandibular condylar cartilage. **J Bone Miner Metab,** v. 21, n. 5, p. 276-86, 2003. ISSN 0914-8779. Disponível em: < https://www.ncbi.nlm.nih.gov/pubmed/12928828 >.

66 ASANO, T. The effects of mandibular retractive force on the growing rat mandible. **Am J Orthod Dentofacial Orthop,** v. 90, n. 6, p. 464-74, Dec 1986. ISSN 0889-5406. Disponível em: < https://www.ncbi.nlm.nih.gov/pubmed/3466527 >.

67 CHARLIER, J. P.; PETROVIC, A. [Studies on the rat mandible in organ culture: does the condylar cartilage have an independent growth potential?]. **Orthod Fr,** v. 38, p. 165-75, 1967. ISSN 0078-6608. Disponível em: < https://www.ncbi.nlm.nih.gov/pubmed/5250143 >.

68 PÉTROVIC, A.; OUDET, C.; GASSON, N. [Effect of devices for mandibular propulsion and retropulsion on the number of serial sarcomeres of the external pterygoid muscle and on the growth of condylar cartilage in young rats]. **Orthod Fr,** v. 44, n. 1, p. 191-212, 1973. ISSN 0078-6608. Disponível em: < https://www.ncbi.nlm.nih.gov/pubmed/4534416 >.

69 CHEN, J. et al. Altered functional loading causes differential effects in the subchondral bone and condylar cartilage in the temporomandibular joint from young mice. **Osteoarthritis Cartilage,** v. 17, n. 3, p. 354-61, Mar 2009. ISSN 1522-9653. Disponível em: < https://www.ncbi.nlm.nih.gov/pubmed/18789726 >.

70 SOBUE, T. et al. Murine TMJ loading causes increased proliferation and chondrocyte maturation. **J Dent Res,** v. 90, n. 4, p. 512-6, Apr 2011. ISSN 1544-0591. Disponível em: < https://www.ncbi.nlm.nih.gov/pubmed/21248355 >.

71 UTREJA, A. et al. Cell and matrix response of temporomandibular cartilage to mechanical loading. **Osteoarthritis Cartilage,** v. 24, n. 2, p. 335-44, Feb 2016. ISSN 1522-9653. Disponível em: < https://www.ncbi.nlm.nih.gov/pubmed/26362410 >.

72 KAUL, R. et al. The Effect of Altered Loading on Mandibular Condylar Cartilage. **PLoS One,** v. 11, n. 7, p. e0160121, 2016. ISSN 1932-6203. Disponível em: < https://www.ncbi.nlm.nih.gov/pubmed/27472059 >.

73 CURTIS, D. A. et al. Adaptability of the adult primate craniofacial complex to asymmetrical lateral forces. **Am J Orthod Dentofacial Orthop,** v. 100, n. 3, p. 266-73, Sep 1991. ISSN 0889-5406. Disponível em: < https://www.ncbi.nlm.nih.gov/pubmed/1877553 >.

74 LIU, C.; KANEKO, S.; SOMA, K. Effects of a mandibular lateral shift on the condyle and mandibular bone in growing rats. **Angle Orthod,** v. 77, n. 5, p. 787-93, Sep 2007. ISSN 0003-3219. Disponível em: < https://www.ncbi.nlm.nih.gov/pubmed/17685779 >.

75 _____. Glenoid fossa responses to mandibular lateral shift in growing rats. **Angle Orthod,** v. 77, n. 4, p. 660-7, Jul 2007. ISSN 0003-3219. Disponível em: < https://www.ncbi.nlm.nih.gov/pubmed/17605490 >.

[76] NAKANO, H. et al. Three-dimensional changes in the condyle during development of an asymmetrical mandible in a rat: a microcomputed tomography study. **Am J Orthod Dentofacial Orthop,** v. 126, n. 4, p. 410-20, Oct 2004. ISSN 0889-5406. Disponível em: < https://www.ncbi.nlm.nih.gov/pubmed/15470344 >.

[77] STOJIĆ, V. et al. Mandibular lateral deviation induces alteration in vascular endothelial growth factor expression and oxidative stress/nitric oxide generation in rat condyle, synovial membrane and masseter muscle. **Arch Oral Biol,** v. 110, p. 104599, Feb 2020. ISSN 1879-1506. Disponível em: < https://www.ncbi.nlm.nih.gov/pubmed/31734543 >.

[78] FUKAYA, S. et al. Possible alternative treatment for mandibular asymmetry by local unilateral IGF-1 injection into the mandibular condylar cavity: Experimental study in mice. **Am J Orthod Dentofacial Orthop,** v. 152, n. 6, p. 820-829, Dec 2017. ISSN 1097-6752. Disponível em: < https://www.ncbi.nlm.nih.gov/pubmed/29173861 >.

[79] ISHII, T.; YAMAGUCHI, H. Influence of extraoral lateral force loading on the mandible in the mandibular development of growing rats. **Am J Orthod Dentofacial Orthop,** v. 134, n. 6, p. 782-91, Dec 2008. ISSN 1097-6752. Disponível em: < https://www.ncbi.nlm.nih.gov/pubmed/19061805 >.

[80] BERESFORD, W. A. Schemes of zonation in the mandibular condyle. **Am J Orthod,** v. 68, n. 2, p. 189-95, Aug 1975. ISSN 0002-9416. Disponível em: < https://www.ncbi.nlm.nih.gov/pubmed/1056706 >.

[81] LIVNE, E.; WEISS, A.; SILBERMANN, M. Changes in growth patterns in mouse condylar cartilage associated with skeletal maturation and senescence. **Growth Dev Aging,** v. 54, n. 4, p. 183-93, 1990. ISSN 1041-1232. Disponível em: < https://www.ncbi.nlm.nih.gov/pubmed/2092017 >.

[82] FLURKEY, K.; CURRER, J. M.; HARRISON, D. E. Mouse Models in Aging Research. In: FOX, J. G.;DAVISSON, M. T.*, et al* (Ed.). **The Mouse in Biomedical Research**. 2nd: Academic Press, v.3, 2007. cap. 20, p.637-672.

[83] DUTTA, S.; SENGUPTA, P. Men and mice: Relating their ages. **Life Sci,** v. 152, p. 244-8, May 2016. ISSN 1879-0631. Disponível em: < https://www.ncbi.nlm.nih.gov/pubmed/26596563 >.

[84] MEAD, T. J.; LEFEBVRE, V. Proliferation assays (BrdU and EdU) on skeletal tissue sections. **Methods Mol Biol,** v. 1130, p. 233-243, 2014. ISSN 1940-6029. Disponível em: < https://www.ncbi.nlm.nih.gov/pubmed/24482177 >.

[85] LI, J.; DONG, S. The Signaling Pathways Involved in Chondrocyte Differentiation and Hypertrophic Differentiation. **Stem Cells Int,** v. 2016, p. 2470351, 2016. ISSN 1687-966X. Disponível em: < https://www.ncbi.nlm.nih.gov/pubmed/28074096 >.

86 RABIE, A. B. et al. The correlation between neovascularization and bone formation in the condyle during forward mandibular positioning. **Angle Orthod,** v. 72, n. 5, p. 431-8, Oct 2002. ISSN 0003-3219. Disponível em: < https://www.ncbi.nlm.nih.gov/pubmed/12401052 >.

87 MAES, C. et al. Osteoblast precursors, but not mature osteoblasts, move into developing and fractured bones along with invading blood vessels. **Dev Cell,** v. 19, n. 2, p. 329-44, Aug 2010. ISSN 1878-1551. Disponível em: < https://www.ncbi.nlm.nih.gov/pubmed/20708594 >.

88 COLNOT, C.; ZHANG, X.; KNOTHE TATE, M. L. Current insights on the regenerative potential of the periosteum: molecular, cellular, and endogenous engineering approaches. **J Orthop Res,** v. 30, n. 12, p. 1869-78, Dec 2012. ISSN 1554-527X. Disponível em: < https://www.ncbi.nlm.nih.gov/pubmed/22778049 >.

89 TULLOCH, J. F. et al. The effect of early intervention on skeletal pattern in Class II malocclusion: a randomized clinical trial. **Am J Orthod Dentofacial Orthop,** v. 111, n. 4, p. 391-400, Apr 1997. ISSN 0889-5406. Disponível em: < https://www.ncbi.nlm.nih.gov/pubmed/9109584 >.

90 KEELING, S. D. et al. Anteroposterior skeletal and dental changes after early Class II treatment with bionators and headgear. **Am J Orthod Dentofacial Orthop,** v. 113, n. 1, p. 40-50, Jan 1998. ISSN 0889-5406. Disponível em: < https://www.ncbi.nlm.nih.gov/pubmed/9457018 >.

91 PANCHERZ, H. The mechanism of Class II correction in Herbst appliance treatment. A cephalometric investigation. **Am J Orthod,** v. 82, n. 2, p. 104-13, Aug 1982. ISSN 0002-9416. Disponível em: < https://www.ncbi.nlm.nih.gov/pubmed/6961781 >.

92 LUND, D. I.; SANDLER, P. J. The effects of Twin Blocks: a prospective controlled study. **Am J Orthod Dentofacial Orthop,** v. 113, n. 1, p. 104-10, Jan 1998. ISSN 0889-5406. Disponível em: < https://www.ncbi.nlm.nih.gov/pubmed/9457025 >.

93 O'BRIEN, K. et al. Effectiveness of early orthodontic treatment with the Twin-block appliance: a multicenter, randomized, controlled trial. Part 1: Dental and skeletal effects. **Am J Orthod Dentofacial Orthop,** v. 124, n. 3, p. 234-43; quiz 339, Sep 2003. ISSN 0889-5406. Disponível em: < https://www.ncbi.nlm.nih.gov/pubmed/12970656 >.

94 YILDIRIM, E.; KARACAY, S.; ERKAN, M. Condylar response to functional therapy with Twin-Block as shown by cone-beam computed tomography. **Angle Orthod,** v. 84, n. 6, p. 1018-25, Nov 2014. ISSN 1945-7103. Disponível em: < https://www.ncbi.nlm.nih.gov/pubmed/24713070 >.

APPENDIX A: FIGURES

a) 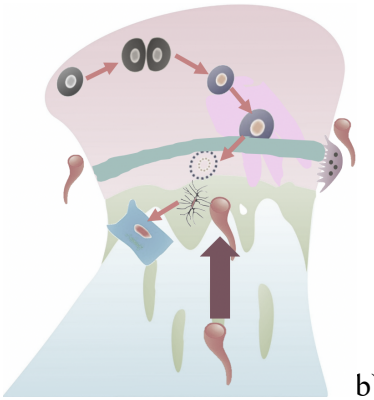 b) 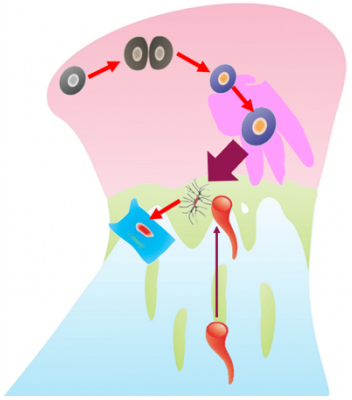

Figure 1: The Central Dogma of Endochondral Ossification and Current Hypothesis

a) The original dogma regarding endochondral illustrates mesenchymal proliferation, differentiation, and growth. A collar of bone inhibits nutrition, resulting in cartilage apoptosis and recruitment of osteoblasts from the underlying blood vessels.
b) The current hypothesis poses that instead of apoptosis and recruitment of osteoblasts from the underlying blood vessels being a primary mechanism for bone development, chondrocytes themselves primarily differentiate into osteoblasts.

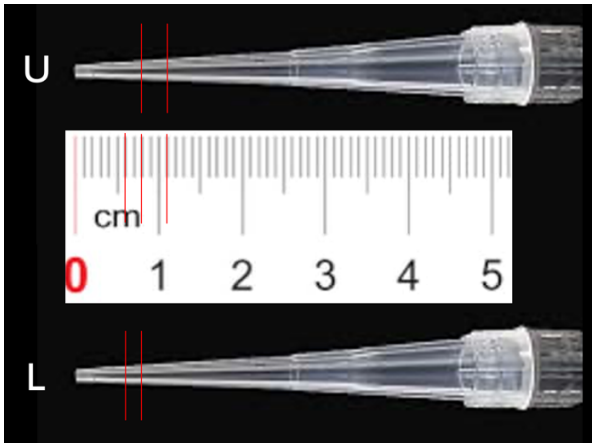


Figure 2: Depiction of Custom Band Creation

Figure 3: Mandibular Deviation Illustration

Photograph depicting shifting mechanism using custom bands to shift the mandibles of the mice to the L. Midline deviation can be noted.

a) 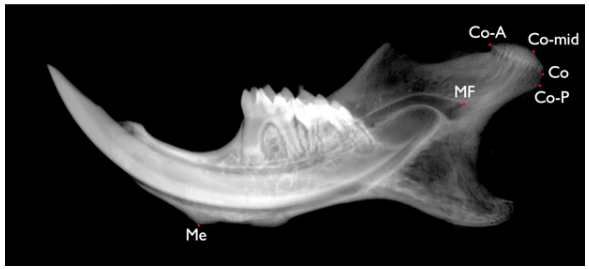

b) 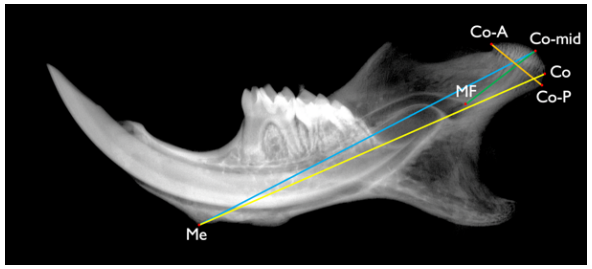


Figure 4: Mandibular 2D Measurements

A) Measurement points: 1) Co-A (anterior condylar articular surface) defined as the most anterior aspect of the radiopaque condylar line; 2) Co (condylion) defined as the most posterior aspect of the radiopaque condylar line; 3) Co-P (posterior condylar surface) defined as the most posterior point of the condylar head and slightly inferior to condylion; 4) Co-mid (condylion mid-point), a point bisecting Co-A and Co-P along the condylar surface; 5) MF (mental foramen) defined as the point in which the radiopaque outline of the superior aspect of the mandibular canal ends; 6) Me (menton) defined as the anterior-inferior point of the mandibular border.

B) Measurement lengths: 1) Mandibular length measured from Co to Me shown in yellow. 2) Mandibular length measured from Co-mid to Me shown in blue. Two different measurements of mandibular length were to reproduce the different ways in which mandibular length has been measured. 3) Condylar length measured from Co-MF shown in green. 4) Condylar AP width measured from Co-A to Co-P shown in orange.

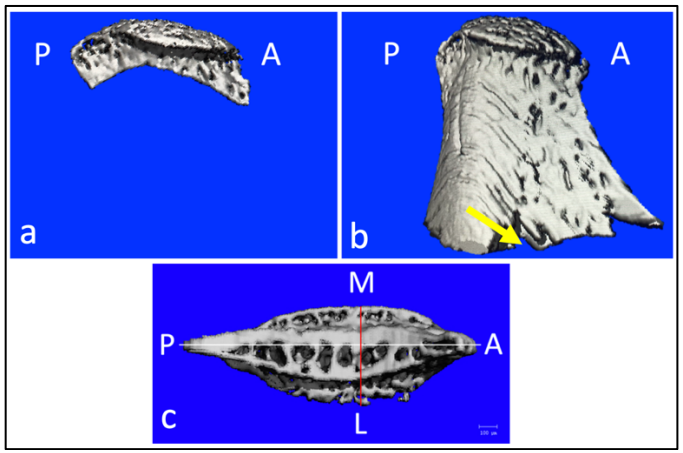


Figure 5: Micro-CT Regions of Interest and Frontal Measurements

a) Three-dimensional rendering of the superior 0.5mm of the condyle, outlined to assess the changes occurring in only the superior aspect of the condyle.
b) Three-dimensional rendering of the entire condylar process outlined. Yellow arrow depicts the general location of the mandibular foramen.
c) Three-dimensional rendering of the inferior aspect of condyle. Condyles were rotated and the medio-lateral width was measured (shown in red) perpendicular to the anterio-posterior plane (shown in white).

a) 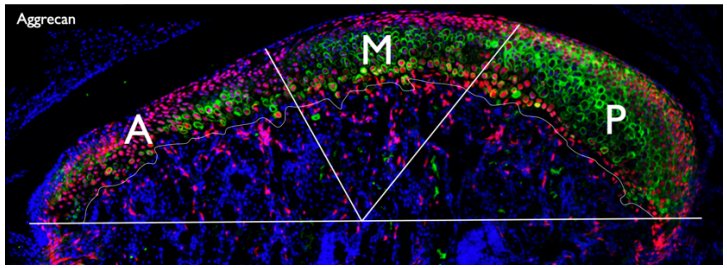

b) 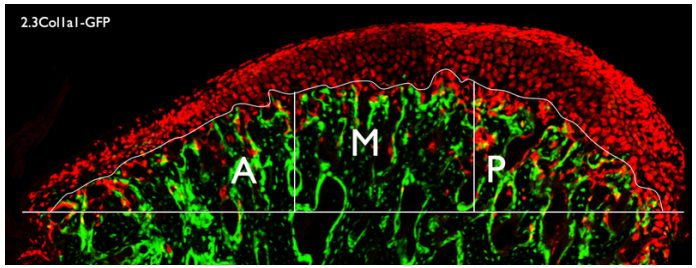


Figure 6: Antero-posterior Subdivision of Histological Slides

The condylar head was bisected at its widest point in the anterior-posterior dimension.

a) The superior segment was cut into three equal parts, segmenting the cartilage into anterior, middle, and posterior segments for chondrogenic analysis.
b) Two perpendicular lines were dropped down from the intersections of the cartilage and bone to subdivide the subchondral bone in anterior, middle, and posterior segments for transdifferentiation analysis.

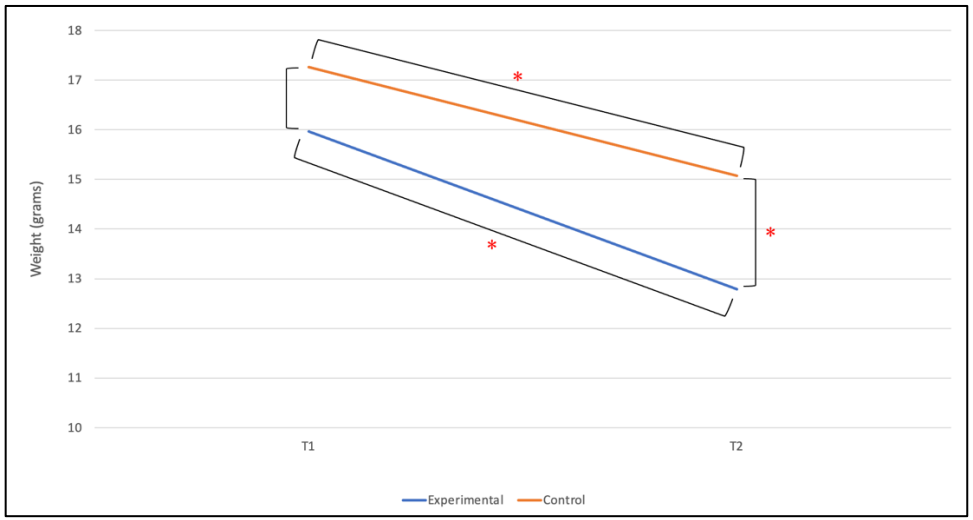


Figure 7: Change in Weight in Grams

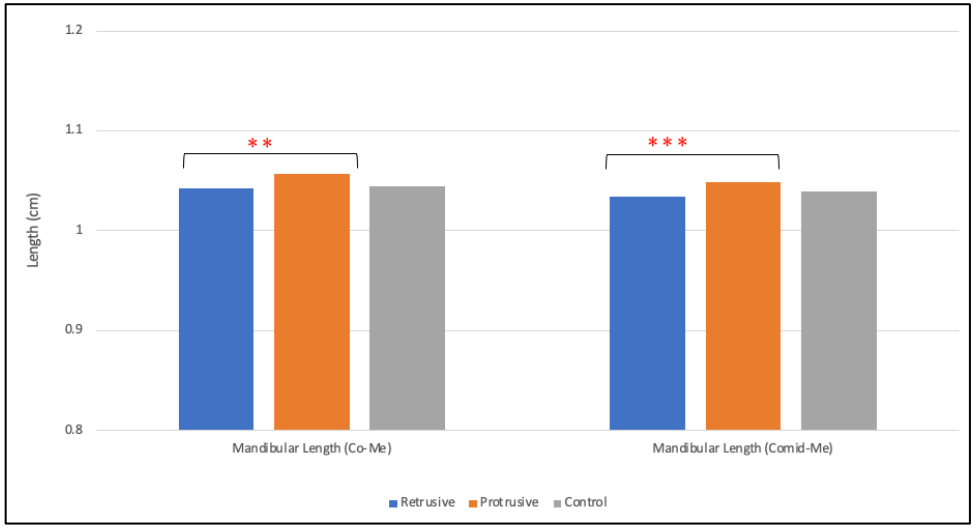


Figure 8: Mandibular Length Differences between the Right and Left Sides of the Experimental Group and the Control Group

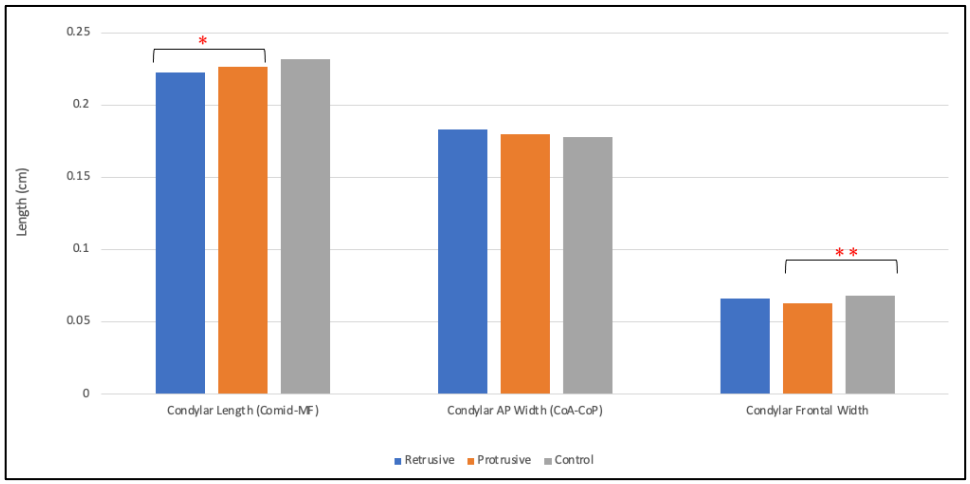


Figure 9: Condylar Length, AP Width, and Frontal Width in Centimeters between the Right and Left Sides of the Experimental Group and the Control Group

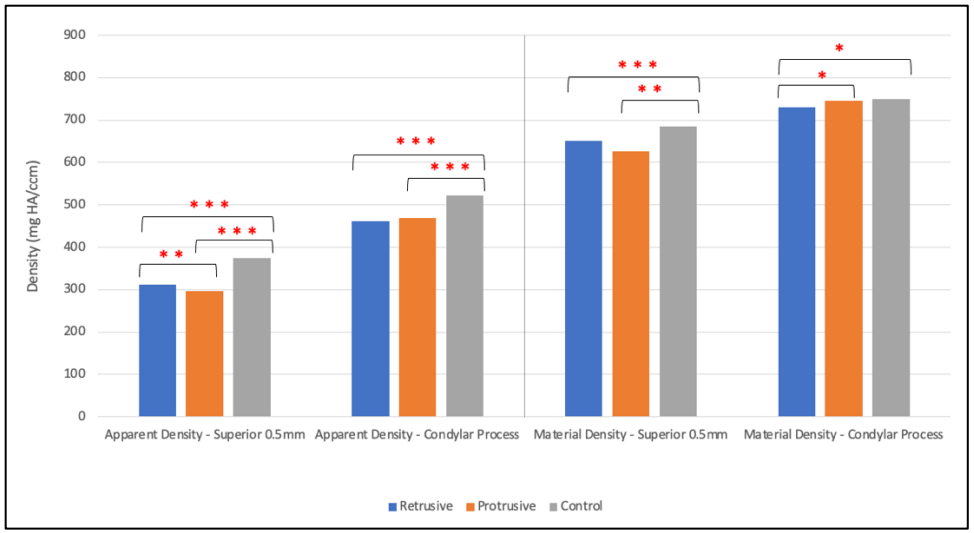


Figure 10: Apparent and Material Density in mgHA/ccm between the Right and Left Sides of the Experimental Group and the Control Group

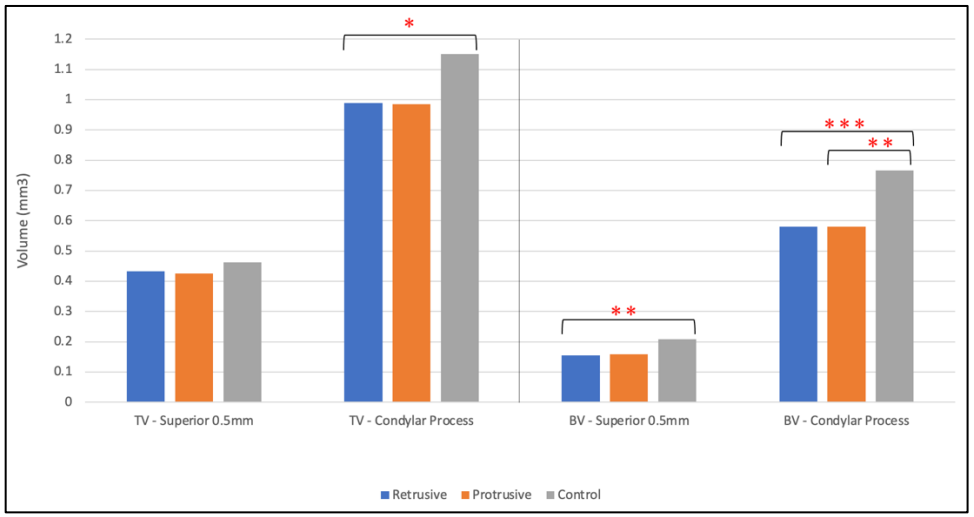


Figure 11: Tissue and Bone Volume in $mm^3$ between the Right and Left Sides of the Experimental Group and the Control Group

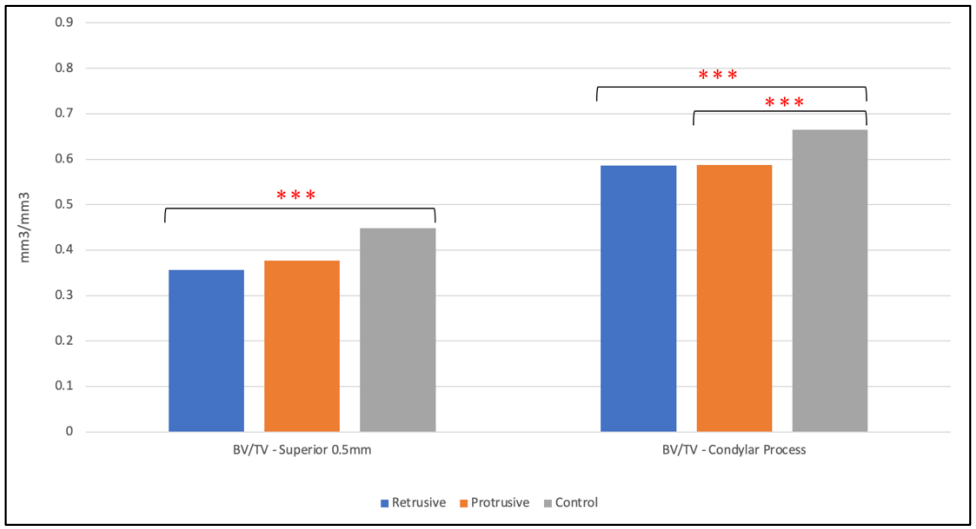


Figure 12: Bone Volume/Tissue Volume in $mm^3/mm^3$ between the Right and Left Sides of the Experimental Group and the Control Group

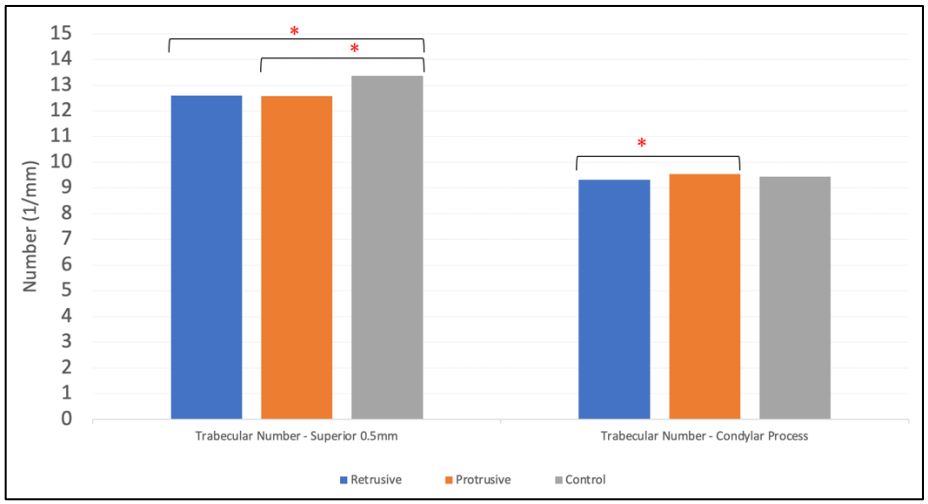


Figure 13: Trabecular Number in 1/mm between the Right and Left Sides of the Experimental Group and the Control Group

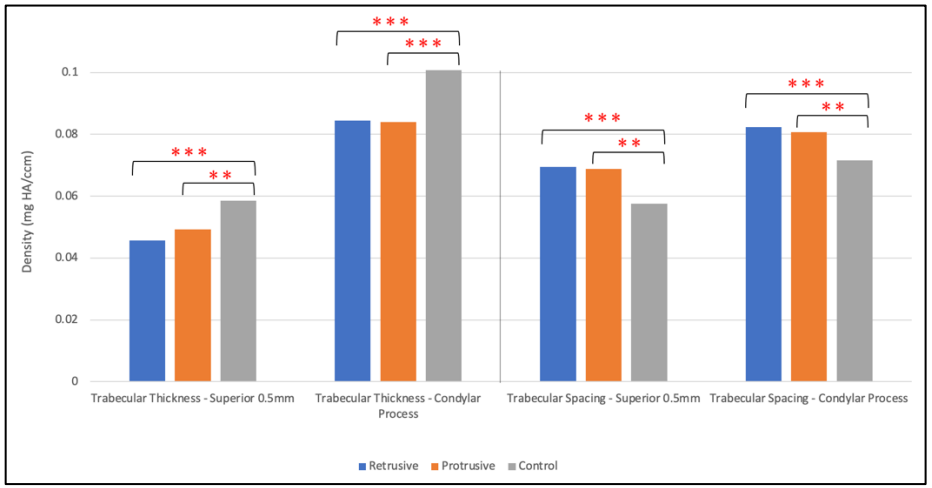


Figure 14: Trabecular Thickness and Spacing in mgHA/ccm between the Right and Left Sides of the Experimental Group and the Control Group

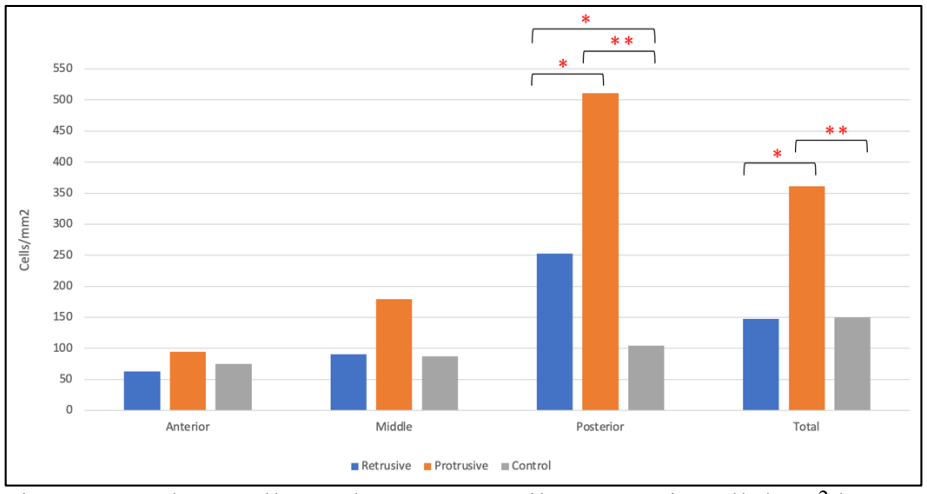


Figure 15: EdU+ Cell Number Over Cartilage Area in cells/mm$^2$ between the Right and Left Sides of the Experimental Group and the Control Group

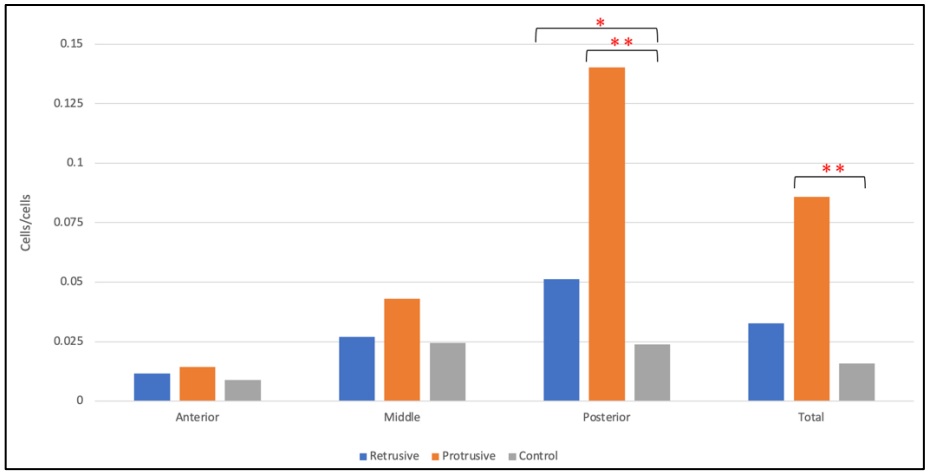


Figure 16: EdU+ Cell Number Over DAPI+ Cell Number in Cartilage (cells/cells) between the Right and Left Sides of the Experimental Group and the Control Group

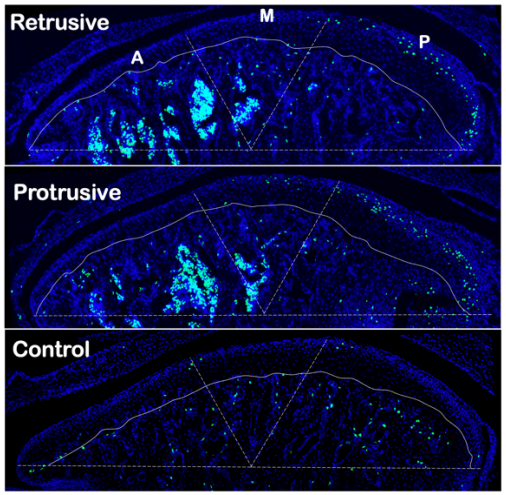


Figure 17: Histological Depiction of EdU+ Cells (Green) and DAPI+ Cells (Blue) in the Condylar Cartilage Between the Right and Left Sides of the Experimental Group and the Control Group

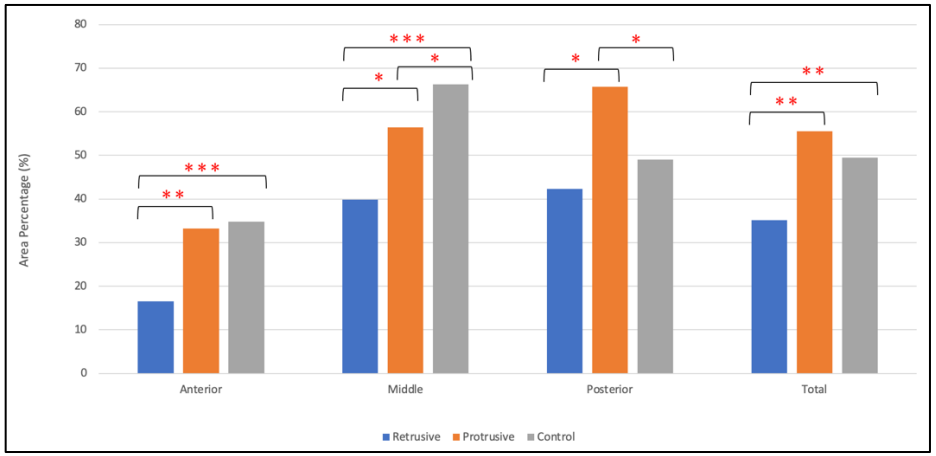


Figure 18: Aggrecan+ Area Over Cartilage Area Percentage (pixels/pixels) between the Right and Left Sides of the Experimental Group and the Control Group

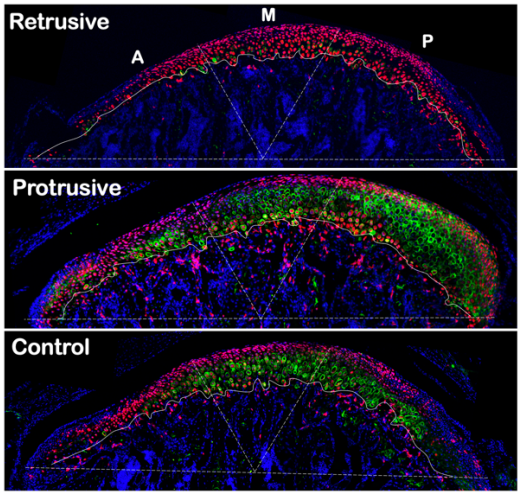


Figure 19: Histological Depiction of Aggrecan+ Cells (Green) in the Condylar Cartilage Between the Right and Left Sides of the Experimental Group and the Control Group

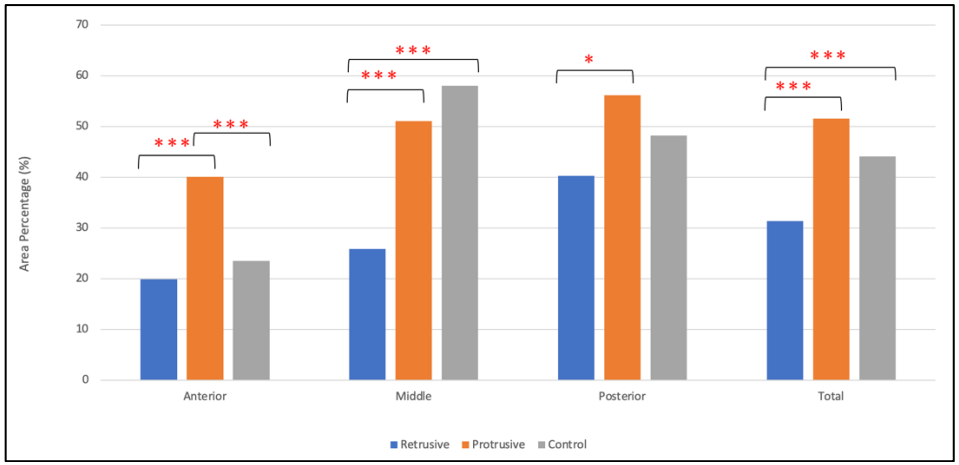


Figure 20: Col10a1+ Area Over Cartilage Area Percentage (pixels/pixels) between the Right and Left Sides of the Experimental Group and the Control Group

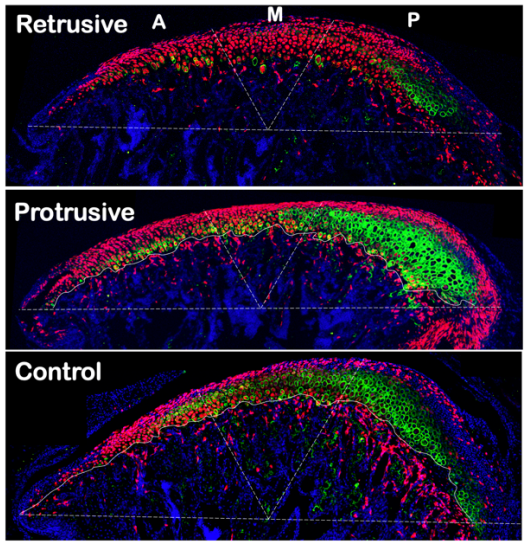


Figure 21: Histological Depiction of Col10a1+ Cells (Green) in the Condylar Cartilage Between the Right and Left Sides of the Experimental Group and the Control Group

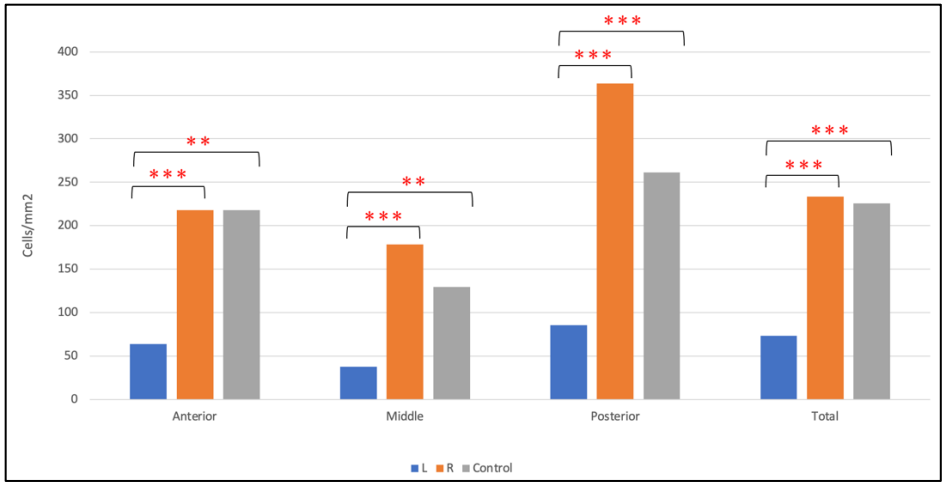


Figure 22: Osx+/Cre+ Cell Number Over Subchondral Bone Area (cells/pixels) between the Right and Left Sides of the Experimental Group and the Control Group

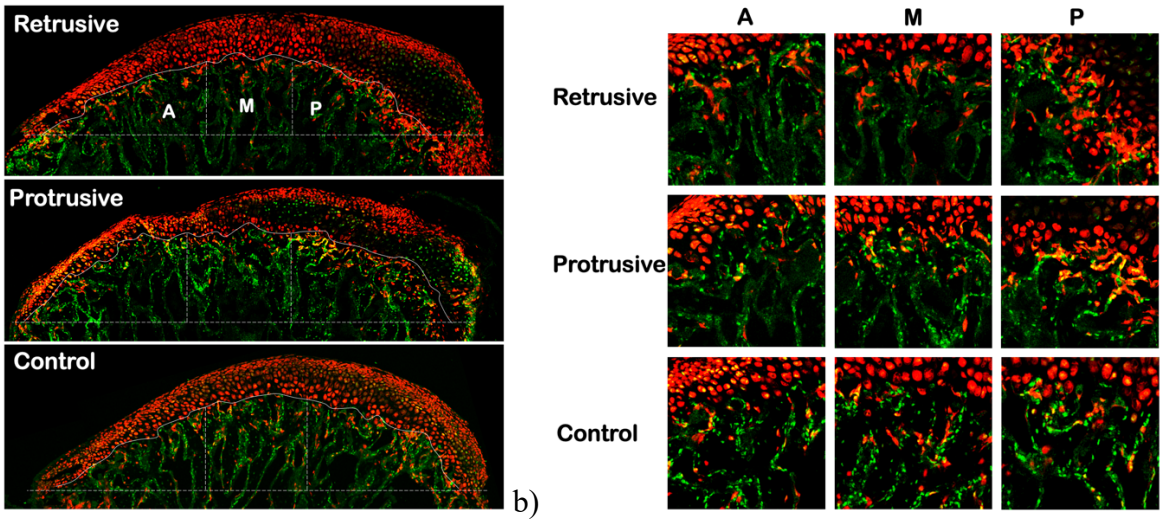


a) b)

Figure 23: Histological Depiction of Cell Transdifferentiation in the Subchondral Bone Between the Right and Left Sides of the Experimental Group and the Control Group

a) Overview with 10x magnification
b) 20x magnification showing cellular changes

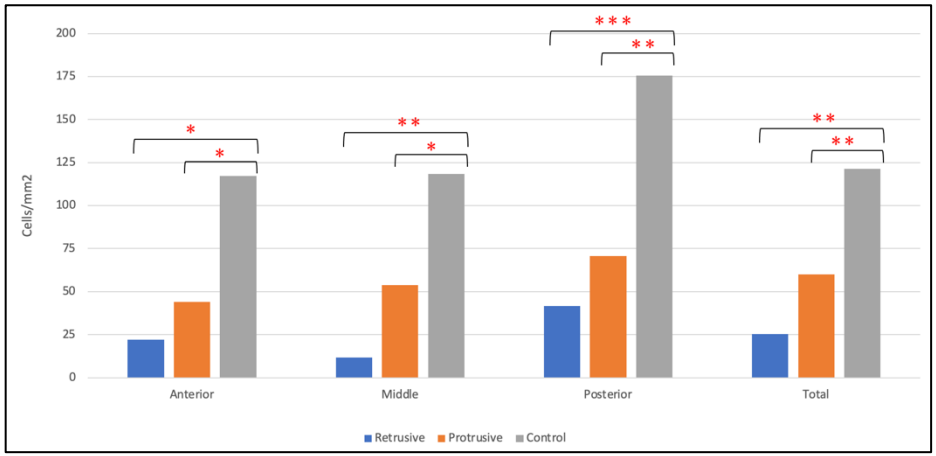


Figure 24: GFP+/Cre+ Cell Number Over Subchondral Bone Area (cells/pixels) between the Right and Left Sides of the Experimental Group and the Control Group

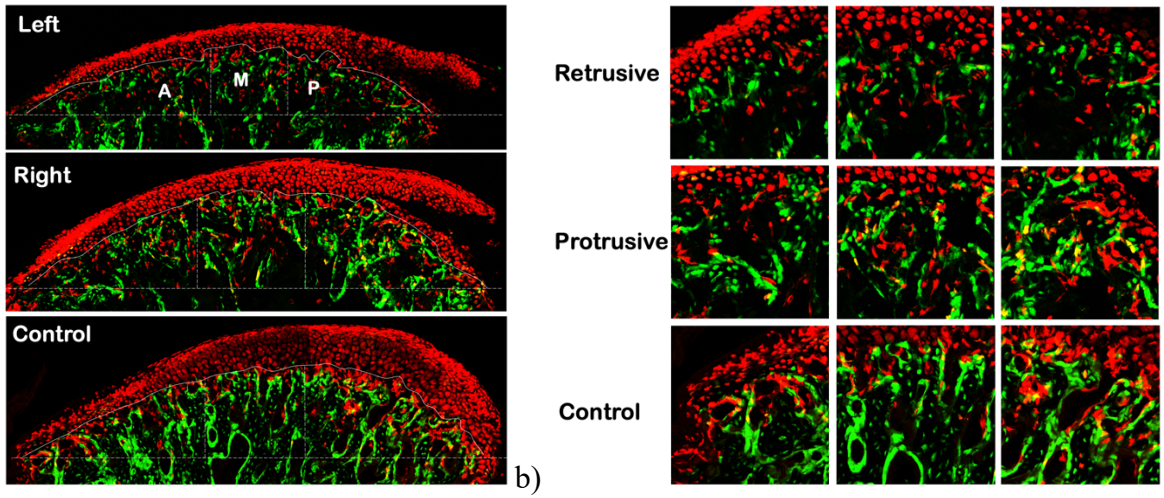


a) b)

Figure 25: Histological Depiction of Cell Transdifferentiation in the Subchondral Bone Between the Right and Left Sides of the Experimental Group and the Control Group

b) Overview with 10x magnification

c) 20x magnification showing cellular changes

# APPENDIX B: TABLES

Table 1: Lateral Deviation Article Summaries ([27; 28; 29; 73; 74; 75; 76; 77; 78; 79])

| Reference | Sample size | Shifting mechanism | Analysis | General results | | |
|---|---|---|---|---|---|---|
| | | | | Retruded (L) | Protruded (R) | Experimental |
| Curtis 1991 | 10 adult rhesus monkeys (3 shifted) | Bilaterally inclined mandibular splints for 6-12 months | Casts, ceph, electromyogram, CT | | ↑ bone density in coronoid process, condyle no dif | ↑ bone density at necks of condyles |
| Fuentes 2003 - I | 39 28-day old male Sprague-Dawley rats | Stainless steel mesh + acrylic around incisors – eval 3, 7, 14 days | Section: AP<br>- eval: condylar thickness, BrdU, Igf-1, Fgf-2 and receptors | ↓ Condylar cartilage thickness<br>↓ BrdU | ↑ Condylar cartilage thickness<br>↑ BrdU | |
| Fuentes 2003 - II | 84 28-day old male Sprague-Dawley rats | Stainless steel mesh + acrylic around incisors – eval 3, 7, 14 days | Semiquantitative reverse-transcription PCR | | At 3 and 7 days:<br>↑ IGF-1/FGF-2 + FGF-R1<br>↓ IGF-1R, FGF-R2, FGF-R3 | Nonprotruded side mimicked controls |
| Nakano 2003 | 10 3-week old male Wistar rats | Inclined crown onto maxillary incisors - eval 21 wks old | Micro-CT | ↑ size/thickness condyle | ↑ mand length<br>↓ BV, BV/TV, Tb.Th, Tb.N<br>Flatter condyle | |
| Nakano 2004 | 60 3-week old male Wistar rats | Metal alloy maxillary occlusal splint – eval 5, 9, 15, 21, 30, 40 wks old | Micro-CT + masseter eval | ↑ ramus height<br>↓ mandible length<br>↑ size/thickness condyle | ↑ mand length<br>↑ mandibular corpus<br>↓ BV of trabeculae, trabecular bone surface, bone-volume fraction, trabecular number<br>↑ bone spacing<br>↓ masseter fiber size | ↓ mandible size<br>↓ ramus height<br>↓ bone volume |
| Sato 2006 | 50 5-week old male Wistar rats: shift, recovery, control | Band covering max incisors eval after 1, 2, 3, 4 wks | Section: ML<br>- Toluidine blue | In lateral region:<br>↓ condylar cartilage thickness<br>↓ BrdU<br>↑ TRAP | In central region:<br>↑ condylar cartilage thickness<br>↑ BrdU<br>↓ TRAP | After appliance removal, results similar to control contralateral<br>↑ BrdU like shifted group still |
| Liu 2007 - Condyle | 48 4-week old male Wistar rats | Maxillary resin plate – eval 2, 4, 8, 23 wks | Section: AP<br>2D x-ray, PAS stain | ↑ condylar AP length<br>↑ ramus height<br>↑ S bone formation<br>↓ P bone formation compared to controls<br>↓ Stutzmann angle | ↑ condylar ML width<br>↑ mand length<br>↑ P bone formation<br>↑ Stutzmann angle | ↓ mandible size |
| Liu 2007 – Glenoid fossa | 96 4-week old male Wistar rats | Resin occlusal plate a metal crown over L incisors | | ↓ fossa size<br>Fossa repositioned P, L, S | Fossa repositioned A, M, I | |
| Ishii 2008 | 30 4-week old male Wistar rats; shift, sham, control | Fixation device fixed bilaterally to zygomatic arch and goes under mandible, OCS connected from device to mand incisor for 2 weeks | Section: ML<br>Micro-CT for 2D, H&E and toluidine blue | Mand length similar to control/sham<br>Chondrocytes shift to M layer<br>Ossification in L direction<br>Man ramus deform toward M | ↑ mandibular length<br>↑ condylar cartilage zone (hypertrophy)<br>↑ erosive zone<br>↓ condylar width | |
| Nakamura 2013 | 18 5-week old male JcI:ICR mice | Band lower incisors, eval every 2 wks until mice 15 wks old | EMG recordings, in-vivo micro-CT | No sig dif 2D measurements | No sig dif 2D measurements | ↓ condylar frontal width<br>↓ bone mineral density |
| Fukaya 2017 | 75 3-week old male JcI:ICR mice | IGF-1 injected into R condyle, eval for 10wks | Section: AP<br>Micro-CT for 2D measurements<br>Real-time PCR | | ↑ mand length<br>↑ condylar cartilage thickness (not S)<br>↑ bone formation (especially A)<br>↑ Col2, Ihh, Runx2, AKTF1, Ki67 | |
| Stojic 2019 | 38 5-week old male Wistar rats | Acrylic resin for 4 wks | Section: AP<br>Micro-CT for 2D measurements, ELISA, Goldner's trichome | ↓ mand length<br>↑ ramus height<br>↓ condylar cartilage, esp. P<br>↑ A + S bone formation<br>↑ VEGF | ↑ mand length<br>↑ P bone formation (but overall less) | ↑ bone marrow cavity area |

Table 2: Lateral Deviation Effects on Condylar and Mandibular Morphology Summary ([27; 28; 29; 73; 74; 75; 76; 77; 78; 79])

| Measurement | Retruded (L) | Protruded (R) | Experimental to Control |
|---|---|---|---|
| Mandibular length (Co-menton) | ↓ (Fukaya, Liu condyle, Nakano 2004/2003, Stojic, Ishii) | ↑ (Fukaya, Liu condyle, Nakano 2004, Stojic 2019, Nakano 2003, Ishii) | No sig dif – both sides (Fukaya), protrusion (Liu condyle, Stojic), retrusion (Ishii)<br>Protruded ↑ (Ishii)<br>Retruded ↓ (Liu condyle, Stojic)<br>Both sides ↓ (Nakano 2004) |
| Mandibular corpus length (posterior point gonial angle menton) | ↓ (Nakano 2004) | ↑ (Nakano 2004) | Both sides ↓ (Nakano 2004) |
| Ramus height (Co superior – mandibular plane) | ↑ (Nakano 2004, Stojic) | No sig dif (Ishii)<br>↑ (Liu – condyle, Stojic) | Both sides ↓ (Liu condyle, Nakano 2004)<br>Protruded ↓ (Stojic) |
| Condylar width | AP: ↑ (Liu condyle)<br>MD (at neck): ↑ (Ishii)<br>No AP/MD spec: Thicker (Nakano 2004) | AP: No sig dif (Fukaya), ↓ (Liu condyle)<br>MD (at neck): ↓ (Ishii) | MD (at neck): ↓ (Ishii)<br>MD: ↓ (Nakamura) |
| Condylar morphology | | Projecting condyle (Fukaya) | |
| Stutzmann angle | ↓ (Liu condyle) | ↑ (Liu condyle)<br>No sig dif (Fukaya) | |
| Size of mandibular fossa | ↓ (Liu fossa) | | |
| Position of mandibular fossa | Posterior, lateral, superior (Liu fossa) | Anterior, medial, inferior (Liu fossa) | |
| Bone density | | | ↓ (Nakamura)<br>↑ at condylar neck (Curtis) |
| Micro-CT measurements | ↑BV, BV/TV, Tb.Th, Tb.N (Nakano 2003/ 2004)<br>↓Tb.Sp (Nakano 2003/2004) | ↓BV, BS, BV/TV, Tb.Th, Tb.N (Nakano 2003, 2004)<br>↑Tb.Sp (Nakano 2003/2004) | ↓BV, BV/TV, Tb.Th (Nakano 2003/2004)<br>↑Tb.Sp, no dif Tb.N (Nakano 2003/2004))<br>↓ trabecular bone (Nakano 2004) |
| Condylar cartilage thickness | ↓ (Fuentes – I)<br>↓, especially P (Stojic)<br>↓, especially on the lateral region (Sato)<br>Shifts to the medial side (Ishii) | ↑ (Fuentes - I, Fukaya (except for superior or middle area), Ishii (increased cartilaginous and erosive zone of cartilage), Sato (esp. central region), Stojic (esp S and P but not sig dif from controls) | |
| Cell proliferation | ↓ BrdU (Fuentes – I)<br>↓ BrdU (↑ relative to controls for lateral 1 week, then significant decrease) (Sato) | ↑ BrdU (Fuentes – I, Sato – particularly central region)<br>↑ Ki67 (Fukaya) | ↑ BrdU on both side relative to controls for first week before retruded decreased and protruded remained higher (Sato) |
| Subchondral bone length | | ↑ (Fukaya) | |
| Subchondral bone formation | ↑superior (Liu condyle)<br>↓posterior (Liu condyle)<br>More lateral direction (Ishii)<br>↑ anterior and superior (Stojic) | ↑posterior (Liu condyle)<br>↑, especially anterior (Fukaya)<br>↑posterior (Stojic) – though overall less than retruded | ↓ in P on retruded side (Liu)<br>↑bone marrow cavities (Stojic) |
| Growth factors | | ↑ IGF-1/FGF-2 (Fuentes – 2)<br>↑VEGF (Stojic) | |
| Chondrogenic markers | | ↑ Col2, Ihh (Fukaya) | |
| Osteogenic markers | | ↑ Runx2 (Fukaya) | |
| Bone resorption markers | ↑ TRAP (Sato) | ↓ TRAP (Sato) | |

Table 3: Means and Standard Deviations (SD) of Weight in Grams at Day 1 and Day 2

| | Experimental | | Control | | |
|---|---|---|---|---|---|
| | Mean | SD | Mean | SD | P value |
| Day 1 | 15.74 | 1.94 | 17.23 | 2.94 | .105 |
| Day 2 | 12.72 | 1.82 | 15.07 | 2.57 | .006 |

Table 4: Means and Standard Deviations (SD) of Two-Dimensional Lengths in Millimeters between the Right and Left Sides of the Experimental Group

| | Left (Retrusive) | | Right (Protrusive) | | L vs. R |
|---|---|---|---|---|---|
| | Mean | SD | Mean | SD | P value |
| Mandibular Length (Co-Me) | 10.42 | 0.18 | 10.57 | 0.25 | .002 |
| Mandibular Length (Comid-Me) | 10.33 | 0.20 | 10.48 | 0.26 | <.001 |
| Condylar Length (Comid-MF) | 2.21 | 0.12 | 2.27 | 0.14 | .039 |
| Condylar AP Width (CoA-CoP) | 1.83 | 0.13 | 1.80 | 0.10 | .471 |
| Condylar Frontal Width | 0.66 | 0.05 | 0.63 | 0.05 | .109 |

Table 5: Means and Standard Deviations (SD) of Two-Dimensional Lengths in Millimeters between the Right and Left Sides of the Experimental Group and the Control Group

| | Left (Retrusive) | | Right (Protrusive) | | Control | | L vs. Cont | R vs. Cont |
|---|---|---|---|---|---|---|---|---|
| | Mean | SD | Mean | SD | Mean | SD | P value | P value |
| Mandibular Length (Co-Me) | 10.43 | 0.19 | 10.57 | 0.25 | 10.44 | 0.27 | .853 | .191 |
| Mandibular Length (Comid-Me) | 10.34 | 0.20 | 10.48 | 0.26 | 10.39 | 0.28 | .558 | .356 |
| Condylar Length (Comid-MF) | 2.23 | 0.13 | 2.27 | 0.14 | 2.32 | 0.18 | .096 | .357 |
| Condylar AP Width (CoA-CoP) | 1.84 | 0.13 | 1.80 | 0.10 | 1.78 | 0.13 | .257 | .613 |
| Condylar Frontal Width | 0.66 | 0.05 | 0.63 | 0.05 | 0.68 | 0.05 | .246 | .010 |

Table 6: Means and Standard Deviations (SD) of Micro-CT Density, Volume, and Trabeculation between the Right and Left Sides of the Experimental Group in the Superior 0.5mm of the Condyle

| | Left (Retrusive) | | Right (Protrusive) | | L vs. R |
|---|---|---|---|---|---|
| | Mean | SD | Mean | SD | P value |
| Apparent Density (mg HA/ccm$^3$) | 311.88 | 18.99 | 296.60 | 18.55 | .001 |
| Material Density (mg HA/ccm$^3$) | 652.92 | 15.83 | 626.39 | 63.12 | .086 |
| Tissue Volume (mm$^3$) | 0.431 | 0.04 | 0.425 | 0.04 | .513 |
| Bone Volume (mm$^3$) | 0.154 | 0.02 | 0.159 | 0.05 | .697 |
| Bone Volume/Tissue Volume (1) | 0.356 | 0.04 | 0.376 | 0.12 | .535 |
| Trabecular Number (1/mm) | 12.51 | 0.73 | 12.57 | 0.82 | .697 |
| Trabecular Thickness (mm) | 0.046 | 0.004 | 0.049 | 0.009 | .214 |
| Trabecular Spacing (mm) | 0.070 | 0.005 | 0.069 | 0.010 | .557 |

Table 7: Means and Standard Deviations (SD) of Micro-CT Density, Volume, and Trabeculation between the Right and Left Sides of the Experimental Group and the Control Group in the Superior 0.5mm of the Condyle (Controlling for Weight)

| | Left (Retrusive) | | Right (Protrusive) | | Control | | L vs. Cont | R vs. Cont |
|---|---|---|---|---|---|---|---|---|
| | Mean | SD | Mean | SD | Mean | SD | P value | P value |
| Apparent Density (mg HA/ccm$^3$) | 311.64 | 20.13 | 296.60 | 18.55 | 373.68 | 24.75 | <.001 | <.001 |
| Material Density (mg HA/ccm$^3$) | 651.32 | 15.93 | 626.39 | 63.12 | 684.98 | 13.39 | <.001 | .005 |
| Tissue Volume (mm$^3$) | 0.433 | 0.04 | 0.425 | 0.04 | 0.462 | 0.06 | .570 | .542 |
| Bone Volume (mm$^3$) | 0.155 | 0.03 | 0.159 | 0.05 | 0.208 | 0.04 | .001 | .065 |
| Bone Volume/Tissue Volume (1) | 0.36 | 0.04 | 0.38 | 0.12 | 0.45 | 0.04 | <.001 | .126 |
| Trabecular Number (1/mm) | 12.60 | 0.75 | 12.57 | 0.82 | 13.37 | 0.72 | .012 | .034 |
| Trabecular Thickness (mm) | 0.046 | 0.004 | 0.049 | 0.009 | 0.059 | 0.005 | <.001 | .012 |
| Trabecular Spacing (mm) | 0.069 | 0.005 | 0.070 | 0.010 | 0.058 | 0.005 | <.001 | .001 |

Table 8: Means and Standard Deviations (SD) of Micro-CT Density, Volume, and Trabeculation between the Right and Left Sides of the Experimental Group in the Condyle Process

| | Left (Retrusive) | | Right (Protrusive) | | L vs. R |
|---|---|---|---|---|---|
| | Mean | SD | Mean | SD | P value |
| Apparent Density (mg HA/ccm$^3$) | 460.96 | 25.82 | 468.73 | 23.04 | .105 |
| Material Density (mg HA/ccm$^3$) | 731.80 | 18.32 | 746.53 | 27.30 | .046 |
| Tissue Volume (mm$^3$) | 0.973 | 0.07 | 0.986 | 0.12 | .670 |
| Bone Volume (mm$^3$) | 0.568 | 0.05 | 0.580 | 0.09 | .553 |
| Bone Volume/Tissue Volume (1) | 0.58 | 0.03 | 0.59 | 0.03 | .554 |
| Trabecular Number (1/mm) | 9.28 | 0.59 | 9.55 | 0.64 | .019 |
| Trabecular Thickness (mm) | 0.084 | 0.008 | 0.084 | 0.007 | .843 |
| Trabecular Spacing (mm) | 0.083 | 0.004 | 0.081 | 0.007 | .106 |

Table 9: Means and Standard Deviations (SD) of Micro-CT Density, Volume, and Trabeculation between the Right and Left Sides of the Experimental Group and the Control Group in the Superior 0.5mm of the Condyle (Controlling for Weight)

| | Left (Retrusive) | | Right (Protrusive) | | Control | | L vs. Cont | R vs. Cont |
|---|---|---|---|---|---|---|---|---|
| | Mean | SD | Mean | SD | Mean | SD | P value | P value |
| Apparent Density (mg HA/ccm$^3$) | 462.19 | 24.80 | 468.73 | 23.04 | 521.66 | 31.43 | <.001 | <.001 |
| Material Density (mg HA/ccm$^3$) | 730.61 | 17.87 | 746.53 | 27.30 | 749.55 | 18.19 | .016 | .651 |
| Tissue Volume (mm$^3$) | 0.989 | 0.08 | 0.986 | 0.12 | 1.151 | 0.18 | .017 | .084 |
| Bone Volume (mm$^3$) | 0.580 | 0.06 | 0.580 | 0.09 | 0.766 | 0.14 | <.001 | .004 |
| Bone Volume/Tissue Volume (1) | 0.59 | 0.03 | 0.59 | 0.03 | 0.66 | 0.04 | <.001 | <.001 |
| Trabecular Number (1/mm) | 9.31 | 0.57 | 9.55 | 0.64 | 9.44 | 0.46 | .605 | .560 |
| Trabecular Thickness (mm) | 0.084 | 0.008 | 0.084 | 0.007 | 0.101 | 0.010 | <.001 | <.001 |
| Trabecular Spacing (mm) | 0.082 | 0.005 | 0.081 | 0.007 | 0.072 | 0.007 | <.001 | .005 |

Table 10: Medians and Interquartile Ranges (IQR) of EdU+ Cell Number Over Cartilage Area (cells/pixels) between the Right and Left Sides of the Experimental Group

| | Left (Retrusive) | | Right (Protrusive) | | L vs. R |
|---|---|---|---|---|---|
| | Median | IQR | Median | IQR | P value |
| Anterior | 62.50 | 27.03, 145.45 | 90.00 | 15.38, 113.64 | .820 |
| Middle | 107.69 | 57.69, 187.50 | 173.91 | 118.64, 297.87 | .140 |
| Posterior | 339.81 | 142.86, 413.61 | 508.20 | 250.00, 655.41 | .017 |
| Total | 196.49 | 113.28, 334.31 | 336.31 | 149.19, 506.93 | .027 |

Table 11: Medians and Interquartile Ranges (IQR) of EdU+ Cell Number Over DAPI+ Cell Number in Cartilage (cells/cells) between the Right and Left Sides of the Experimental Group

| | Left (Retrusive) | | Right (Protrusive) | | L vs. R |
|---|---|---|---|---|---|
| | Median | IQR | Median | IQR | P value |
| Anterior | 0.014 | 0.004, 0.031 | 0.013 | 0.004, 0.028 | .733 |
| Middle | 0.031 | 0.016, 0.058 | 0.043 | 0.022, 0.120 | .334 |
| Posterior | 0.073 | 0.026, 0.125 | 0.140 | 0.055, 0.184 | .088 |
| Total | 0.039 | 0.021, 0.123 | 0.079 | 0.033, 0.125 | .211 |

Table 12: Medians and Interquartile Ranges (IQR) of EdU+ Cell Number Over Cartilage Area (cells/pixels) between the Right and Left Sides of the Experimental Group and the Control Group

| | Left (Retrusive) | | Right (Protrusive) | | Control | | L vs. Cont | R vs. Cont |
|---|---|---|---|---|---|---|---|---|
| | Median | IQR | Median | IQR | Median | IQR | P value | P value |
| Anterior | 62.50 | 26.17, 134.13 | 94.38 | 15.71, 167.69 | 75.00 | 16.13, 155.17 | .748 | .890 |
| Middle | 90.91 | 64.56, 182.79 | 179.26 | 123.07, 291.59 | 87.50 | 74.63, 214.29 | .763 | .192 |
| Posterior | 253.01 | 134.59, 407.56 | 511.24 | 260.23, 652.07 | 104.17 | 75.27, 307.69 | .015 | .002 |
| Total | 147.29 | 109.78, 294.31 | 361.19 | 153.03, 488.13 | 149.61 | 59.76, 219.51 | .168 | .006 |

Table 13: Medians and Interquartile Ranges (IQR) of EdU+ Cell Number Over DAPI+ Cell Number in Cartilage (cells/cells) between the Right and Left Sides of the Experimental Group and the Control Group

| | Left (Retrusive) | | Right (Protrusive) | | Control | | L vs. Cont | R vs. Cont |
|---|---|---|---|---|---|---|---|---|
| | Median | IQR | Median | IQR | Median | IQR | P value | P value |
| Anterior | 0.012 | 0.004, 0.030 | 0.014 | 0.004, 0.034 | 0.009 | 0.003, 0.026 | .545 | .452 |
| Middle | 0.027 | 0.015, 0.053 | 0.043 | 0.022, 0.115 | 0.024 | 0.018, 0.035 | .748 | .133 |
| Posterior | 0.051 | 0.025, 0.124 | 0.140 | 0.056, 0.179 | 0.024 | 0.015, 0.064 | .027 | .002 |
| Total | 0.033 | 0.021, 0.099 | 0.086 | 0.034, 0.120 | 0.016 | 0.015, 0.047 | .086 | .002 |

Table 14: Means and Standard Deviations (SD) of Aggrecan+ Area Over Cartilage Area Percentage (pixels/pixels) between the Right and Left Sides of the Experimental Group

| | Left (Retrusive) | | Right (Protrusive) | | L vs. R |
|---|---|---|---|---|---|
| | Mean | SD | Mean | SD | P value |
| Anterior | 18.67 | 10.14 | 33.26 | 17.27 | .006 |
| Middle | 41.28 | 18.46 | 56.42 | 16.26 | .013 |
| Posterior | 47.91 | 26.26 | 65.74 | 22.18 | .011 |
| Total | 39.21 | 18.45 | 55.58 | 16.97 | .002 |

Table 15: Means and Standard Deviations (SD) of Aggrecan+ Area Over Cartilage Area Percentage (pixels/pixels) between the Right and Left Sides of the Experimental Group and the Control Group

| | Left (Retrusive) | | Right (Protrusive) | | Control | | L vs. Cont | R vs. Cont |
|---|---|---|---|---|---|---|---|---|
| | Mean | SD | Mean | SD | Mean | SD | P value | P value |
| Anterior | 16.52 | 10.34 | 33.26 | 17.27 | 34.82 | 13.91 | <.001 | .791 |
| Middle | 39.90 | 19.12 | 56.42 | 16.26 | 66.34 | 7.58 | <.001 | .042 |
| Posterior | 42.27 | 26.39 | 65.74 | 22.18 | 49.07 | 10.40 | .326 | .020 |
| Total | 35.13 | 18.86 | 55.58 | 16.97 | 49.49 | 7.36 | .007 | .232 |

Table 16: Means and Standard Deviations (SD) of Col10a1+ Area Over Cartilage Area Percentage (pixels/pixels) between the Right and Left Sides of the Experimental Group

| | Left (Retrusive) | | Right (Protrusive) | | L vs. R |
|---|---|---|---|---|---|
| | Mean | SD | Mean | SD | P value |
| Anterior | 17.15 | 9.16 | 40.07 | 10.38 | <.001 |
| Middle | 23.15 | 11.12 | 51.02 | 17.46 | <.001 |
| Posterior | 40.37 | 11.93 | 56.17 | 18.01 | .017 |
| Total | 30.01 | 8.91 | 51.51 | 13.63 | <.001 |

Table 17: Means and Standard Deviations (SD) of Col10a1+ Area Over Cartilage Area Percentage (pixels/pixels) between the Right and Left Sides of the Experimental Group and the Control Group

| | Left (Retrusive) | | Right (Protrusive) | | Control | | L vs. Cont | R vs. Cont |
|---|---|---|---|---|---|---|---|---|
| | Mean | SD | Mean | SD | Mean | SD | P value | P value |
| Anterior | 19.91 | 11.68 | 40.07 | 10.38 | 23.48 | 6.59 | .301 | <.001 |
| Middle | 25.85 | 14.83 | 51.02 | 17.46 | 57.97 | 10.40 | <.001 | .200 |
| Posterior | 40.29 | 11.81 | 56.17 | 18.01 | 48.20 | 12.15 | .068 | .171 |
| Total | 31.31 | 9.39 | 51.51 | 13.63 | 44.12 | 7.15 | <.001 | .086 |

Table 18: Medians and Interquartile Ranges (IQR) of Osx+/Cre+ Cell Number Over Subchondral Bone Area (cells/pixels) between the Right and Left Sides of the Experimental Group

| | Left (Retrusive) | | Right (Protrusive) | | L vs. R |
|---|---|---|---|---|---|
| | Median | IQR | Median | IQ R | P value |
| Anterior | 65.91 | 40.40, 113.52 | 192.18 | 106.71, 402.75 | .002 |
| Middle | 38.80 | 26.97, 99.78 | 171.43 | 94.65, 215.52 | .008 |
| Posterior | 98.12 | 36.37, 160.47 | 337.82 | 171.44, 458.89 | .004 |
| Total | 74.17 | 34.01, 127.74 | 208.60 | 148.12, 308.16 | .004 |

Table 19: Medians and Interquartile Ranges (IQR) of Osx+/Cre+ Cell Number Over Subchondral Bone Area (cells/pixels) between the Right and Left Sides of the Experimental Group and the Control Group

| | Left (Retrusive) | | Right (Protrusive) | | Control | | L vs. Cont | R vs. Cont |
|---|---|---|---|---|---|---|---|---|
| | Median | IQR | Median | IQR | Median | IQR | P value | P value |
| Anterior | 63.64 | 41.67, 107.91 | 217.69 | 117.11, 472.60 | 218.11 | 90.70, 300.31 | .001 | .771 |
| Middle | 37.59 | 26.79, 65.79 | 178.29 | 107.55, 225.09 | 129.31 | 66.78, 207.16 | .001 | .244 |
| Posterior | 85.71 | 37.38, 151.52 | 363.64 | 172.82, 451.76 | 261.19 | 170.38, 415.55 | <.001 | .497 |
| Total | 73.39 | 42.95, 108.53 | 233.67 | 158.46, 354.24 | 225.73 | 116.94, 279.65 | <.001 | .497 |

Table 20: Medians and Interquartile Ranges (IQR) of 2.3Col1a1-GFP+/Cre+ Cell Number Over Subchondral Bone Area (cells/pixels) between the Right and Left Sides of the Experimental Group

| | Left (Retrusive) | | Right (Protrusive) | | L vs. R |
|---|---|---|---|---|---|
| | Median | IQR | Median | IQ R | P value |
| Anterior | 33.72 | 12.97, 109.98 | 36.87 | 20.50, 77.35 | .754 |
| Middle | 12.46 | 4.48, 85.24 | 46.30 | 14.99, 70.78 | .388 |
| Posterior | 47.35 | 18.83, 102.66 | 67.46 | 30.32, 166.36 | .272 |
| Total | 25.36 | 19.14, 101.06 | 54.06 | 22.98, 105.16 | .433 |

Table 21: Medians and Interquartile Ranges (IQR) of 2.3Col1a1-GFP+/Cre+ Cell Number Over Subchondral Bone Area (cells/pixels) between the Right and Left Sides of the Experimental Group and the Control Group

| | Left (Retrusive) | | Right (Protrusive) | | Control | | L vs. Cont | R vs. Cont |
|---|---|---|---|---|---|---|---|---|
| | Median | IQR | Median | IQR | Median | IQR | P value | P value |
| Anterior | 21.98 | 12.50, 116.07 | 44.12 | 21.13, 106.54 | 117.15 | 45.03, 313.90 | .016 | .047 |
| Middle | 11.76 | .00, 56.45 | 53.85 | 17.40, 109.69 | 118.45 | 46.28, 225.19 | .002 | .042 |
| Posterior | 41.67 | 21.28, 93.33 | 70.71 | 35.65, 162.85 | 175.43 | 101.92, 304.33 | <.001 | .029 |
| Total | 25.21 | 17.24, 71.05 | 60.00 | 27.82, 130.90 | 121.38 | 69.74, 283.18 | .001 | .029 |